SARS-CoV-2 vaccination enhances the effector qualities of spike-specific T cells induced by COVID-19

Authors

Curtis Cai[1,*,†], Yu Gao[1,†], Sarah Adamo[1], Olga Rivera-Ballesteros[1], Lotta Hansson[2,3], Anders Österborg[2,3], Peter Bergman[4,5], Johan K. Sandberg[1], Hans-Gustaf Ljunggren[1], Niklas Björkström[1], Kristoffer Strålin[6], Sian Llewellyn-Lacey[7], David A. Price[7,8], Chuan Qin[9,10], Alba Grifoni[11], Daniela Weiskopf[11], E. John Wherry[12,13,14], Alessandro Sette[11,15], Soo Aleman[6,16], Marcus Buggert[1,*]

Affiliations

[1]Department of Medicine Huddinge, Center for Infectious Medicine, Karolinska Institutet, Karolinska University Hospital, Stockholm, Sweden

[2]Department of Hematology, Karolinska University Hospital, Stockholm, Sweden

[3]Department of Oncology-Pathology, Karolinska Institutet, Stockholm, Sweden

[4]Department of Laboratory Medicine, Karolinska Institutet, Stockholm, Sweden

[5]Department of Clinical Immunology and Transfusion Medicine, Karolinska University Hospital, Stockholm, Sweden

[6]Department of Infectious Diseases, Karolinska University Hospital, Stockholm, Sweden

[7]Division of Infection and Immunity, Cardiff University School of Medicine, University Hospital of Wales, Cardiff, UK

[8]Systems Immunity Research Institute, Cardiff University School of Medicine, University Hospital of Wales, Cardiff, UK

[9]Beijing Key Laboratory for Animal Models of Emerging and Reemerging Infectious Diseases, Institute of Laboratory Animal Science, Chinese Academy of Medical Sciences, Beijing, China

[10]National Health Commission Key Laboratory of Human Disease Comparative Medicine, Comparative Medicine Center, Peking Union Medical College, Beijing, China

[11]Center for Infectious Disease and Vaccine Research, La Jolla Institute for Immunology, La Jolla, California, USA

[12]Institute for Immunology, Perelman School of Medicine at the University of Pennsylvania, Pennsylvania, USA

[13]Department of Systems Pharmacology and Translational Therapeutics, Perelman School of Medicine at the University of Pennsylvania, Pennsylvania, USA

[14]Parker Institute for Cancer Immunotherapy, Perelman School of Medicine at the University of Pennsylvania, Pennsylvania, USA

[15]Department of Medicine, Division of Infectious Diseases and Global Public Health, University of California, San Diego, California, USA

[16]Department of Medicine Huddinge, Infectious Diseases, Karolinska Institutet, Stockholm, Sweden

†These authors contributed equally to this work.

*Correspondence should be addressed to Curtis Cai (Curtis.Cai@ki.se) or Marcus Buggert (Marcus.Buggert@ki.se).

ABSTRACT

T cells are critical for immune protection against severe COVID-19. It has nonetheless remained unclear whether repeated exposure to SARS-CoV-2 antigens delivered in the context of vaccination fuels T cell exhaustion or reshapes T cell functionality. Here, we sampled convalescent donors with a history of mild or severe COVID-19 before and after SARS-CoV-2 vaccination to profile the functional spectrum of hybrid T cell immunity. Using combined single-cell technologies and high-dimensional flow cytometry, we found that the frequencies and functional capabilities of spike-specific $CD4^+$ and $CD8^+$ T cells in previously infected individuals were enhanced by vaccination, despite concomitant increases in the expression of inhibitory receptors, such as PD-1 and TIM3. In contrast, $CD4^+$ and $CD8^+$ T cells targeting non-spike proteins remained functionally static and waned over time, and only minimal effects were observed in healthy vaccinated donors experiencing breakthrough infections with SARS-CoV-2. Moreover, hybrid immunity was characterized by elevated expression of IFN-γ, which was linked with clonotype specificity in the $CD8^+$ T cell lineage. Collectively, these findings identify a molecular hallmark of hybrid immunity and suggest that vaccination after infection is associated with cumulative immunological benefits over time, potentially conferring enhanced protection against subsequent episodes of COVID-19.

One Sentence Summary

SARS-CoV-2 vaccination enhances spike-specific T cell functionality after COVID-19.

INTRODUCTION

Natural infection with severe acute respiratory syndrome coronavirus 2 (SARS-CoV-2) elicits T cell responses against all regions of the viral proteome (*1*). In contrast, globally adopted vaccination methods focus immune responses on the spike protein alone, primarily aiming to elicit antibodies that neutralize SARS-CoV-2. Accordingly, the combination of infection and vaccination elicits T cell responses against the spike protein and non-spike proteins (*2*), encompassed within the term hybrid immunity. In retrospective comparisons with previously infected but unvaccinated individuals, hybrid immunity has been associated with lower rates of reinfection (*3*) and lower rates of hospitalization after reinfection (*4*), and durable protection against severe disease has largely been maintained despite the emergence of Omicron (*5*). These observations suggest that hybrid immunity is likely characterized by long-term memory against SARS-CoV-2.

Recurrent antigen exposure in the context of booster vaccination (*6*) or hybrid immunity (*2, 7, 8*) has been shown to increase the frequencies of spike-specific T cells in the circulation. Earlier studies nonetheless suggested that repetitive stimulation could lead to T cell dysfunction, especially after severe infection, which has been associated with peripheral lymphopenia (*9*), higher frequencies of SARS-CoV-2-specific T cells during convalescence (*10*), and signatures of exhaustion compared with other forms of pneumonia that require hospitalization (*11*). However, elevated expression of exhaustion markers, such as PD-1, does not necessarily equate with T cell dysfunction (*12*) and may instead serve as a sign of activation during acute infection. In separate transcriptomic analyses, T cell expression of exhaustion markers was largely equivalent in healthy donors and patients hospitalized with acute COVID-19 (*13*), and among $CD8^+$ T cells targeting SARS-CoV-2, exhaustion signatures were more pronounced in donors with mild versus severe disease (*14*). It has also been shown that mRNA vaccination induces polyfunctional (*15*) and durable (*16*) T cell responses more homogenously than infection, and given a previous report indicating that $CD4^+$ T cells coexpressing interferon (IFN)-γ and interleukin (IL)-10 can arise in the

context of hybrid immunity but not after vaccination alone (*17*), it seems plausible that mRNA vaccination could alter the landscape of established T cell immunity.

Individuals with immunological memory formed during the first pandemic wave of infections (early 2020) and subsequently boosted by vaccination (early 2021) represent a unique case of hybrid immunity generated via recurrent exposure to the same ancestral Wuhan strain of SARS-CoV-2. We took advantage of this scenario to determine how recurrent stimulation with an identical antigen impacts the frequencies and functional capabilities of $CD4^+$ and $CD8^+$ T cells targeting the spike protein of SARS-CoV-2. Using *ex vivo* stimulations, high-dimensional flow cytometry, and single-cell RNA-sequencing (scRNA-seq), we identified IFN-γ upregulation as the most consistent and robust signature of hybrid $CD4^+$ and $CD8^+$ T cell immunity.

RESULTS

Vaccination increases spike-specific T cell frequencies after infection with SARS-CoV-2

To investigate the potential utility of vaccination after infection with SARS-CoV-2, we first evaluated virus-specific T cell immunity in donors with a confirmed history of mild (non-hospitalized) or severe (hospitalized) COVID-19. Samples of peripheral blood were collected in December 2020 or January 2021, 6–9 months into convalescence (6–9M), and in October 2021, 18 months into convalescence (18M). Matched samples were acquired from 31 donors with a history of mild disease (total $n = 50$) and 24 donors with a history of severe disease (total $n = 53$) (Fig. 1A and table S1). All 6–9M donors were sampled before vaccination was available, and most 18M donors were vaccinated twice between May and August 2021 (mRNA, 52/69; viral vector, 2/69; unknown platform, 5/69; unvaccinated, 10/69) (Fig. 1B and table S1), allowing us to characterize hybrid immunity. Four overlapping peptide pools spanning the spike, nucleocapsid, combined membrane and envelope, and combined open reading frame (ORF) proteins 3–10 were used to assess the functional phenotype of SARS-CoV-2-specific T cells in an activation-induced marker (AIM) assay (Fig. 1A).

At both time points, SARS-CoV-2-specific $CD4^+$ T cells identified via coexpression of CD69 and CD40L (Fig. 1C and fig. S1A) were more abundant in donors with severe disease versus mild disease across all tested regions of the viral proteome (Fig. 1D and fig. S1B), consistent with a previous study (*10*). The effect of vaccination was also evident. $CD4^+$ T cell responses directed against the spike protein increased significantly in magnitude after vaccination, whereas $CD4^+$ T cell responses directed against other viral proteins remained unchanged or even decreased in magnitude, irrespective of vaccination (Fig. 1E and fig. S2A). Similar patterns were observed for spike-specific $CD8^+$ T cells identified via coexpression of CD69 and 4-1BB (Fig. 1F and fig. S1A). In particular, higher frequencies of spike-specific $CD8^+$ T cells were detected in donors with severe

versus mild disease, and subsequent vaccination increased the frequencies of spike-specific $CD8^+$ T cells, irrespective of initial disease severity (Fig. 1G and fig. S2B).

These findings demonstrate that vaccination augments spike-specific $CD4^+$ and $CD8^+$ T cell frequencies elicited by natural infection with SARS-CoV-2.

Vaccination reshapes the effector qualities of spike-specific T cells induced by COVID-19

To investigate the functionality of spike-specific $CD4^+$ T cells after natural infection and subsequent vaccination, we measured the intracellular production of IFN-γ, IL-2, and tumor necrosis factor (TNF) in response peptide stimulation (Fig. 2A). TNF was the predominant function elicited among spike-specific $CD4^+$ T cells at both time points, with slightly lower levels of IL-2 and IFN-γ (Fig. 2B), and the proportion of triple-positive cells increased significantly in vaccinated donors at 18M (Fig. 2B). Spike-specific $CD4^+$ T cell polyfunctionality also increased from 6–9M to 18M (Fig. 2C). In contrast, only minor shifts in polyfunctionality were observed among nucleocapsid-specific $CD4^+$ T cells, and no significant changes in polyfunctionality were observed among $CD4^+$ T cells targeting the combined membrane and envelope proteins or ORF3–10 (Fig. 2C). Of note, robust polyfunctionality was observed before and after vaccination in donors with a history of severe COVID-19, arguing against the occurrence of imprints causing T cell dysfunction long after infection with SARS-CoV-2 (Fig. 2C and fig. S3A).

$CD8^+$ T cell responses were assessed similarly using IFN-γ as a marker of antigen specificity after stimulation with a pool of peptides representing immunodominant epitopes from the spike protein of SARS-CoV-2 (Fig. 2D). The proportions of monofunctional IFN-γ^+ spike-specific $CD8^+$ T cells remained unchanged over time (fig. S3B), whereas the proportions of spike-specific $CD8^+$ T cells that coexpressed IFN-γ, TNF, and granzyme B (GzmB) increased at 18M (Fig. 2E). Of note, IFN-γ^+ spike-specific $CD8^+$ T cell frequencies decreased in donors with a history of mild disease but

increased in donors with a history of severe disease, indicating a dichotomous effect of vaccination (Fig. 2E).

Recurrent antigen exposure can lead to the upregulation of inhibitory receptors, potentially resulting in T cell exhaustion (*18*). To investigate this possibility, we used human leukocyte antigen class I (HLA-I) tetramers to identify SARS-CoV-2 spike-specific, SARS-CoV-2 non-spike-specific, and CMV-specific $CD8^+$ T cells in the absence of peptide stimulation (Fig. 2F and table S2), simultaneously analyzing surface expression of the exhaustion markers PD-1, TIM3, LAG3, and TIGIT (fig. S3C). The proportions of spike-specific $CD8^+$ T cells expressing PD-1 and TIM3 increased after vaccination (Fig. 2, G and H), whereas the proportions of proportions of spike-specific $CD8^+$ T cells expressing LAG3 and TIGIT remained unchanged after vaccination (fig. S3D). No changes in inhibitory receptor expression were detected among non-spike-specific or CMV-specific $CD8^+$ T cells after vaccination (Fig. 2H and fig. S3D).

These results show that vaccination enhances the functional qualities of spike-specific $CD4^+$ and $CD8^+$ T cells induced by natural infection with SARS-CoV-2, despite the upregulation of inhibitory receptors often associated with exhaustion.

Single-cell analysis defines the granularity of hybrid spike-specific T cell immunity

To extend these findings, we performed scRNA-seq in conjunction with oligo-conjugated antibody staining (CITE-seq) and T cell receptor sequencing (TCR-seq) to profile the global landscape of hybrid immunity. AIM^+ $CD4^+$ and $CD8^+$ T cells were sorted via flow cytometry and processed for scRNA-seq from a previously infected donor sampled before and soon after vaccination, recently infected convalescent donors sampled on day 35 only (n = 3), and donors with a history of mild (n = 3) or severe (n = 3) COVID-19 sampled at 6–9M and 18M (Fig. 3A, fig. S4A, and table S3). We identified five clusters of conventional $CD4^+$ and $CD8^+$ T cells after dimensionality reduction

via Uniform Manifold Approximation and Projection (UMAP) (Fig. 3, B and C) and the exclusion of NK cells, MAIT cells, γδ T cells, and NKT cells (fig. S4, B to E). Each cluster incorporated cells from each participant group and time point (Fig. 3D and fig. S4F). In general, the frequencies of spike-specific $CD4^+$ and $CD8^+$ T cells increased after vaccination, although it should be noted that our sorting strategy was unable to exclude bystander-activated cells or the small fractions of AIM^+ cells that were detectable in the absence of peptide stimulation (fig. S4G).

The largest $CD4^+$ T cell cluster (cluster 0) was characterized by effector signatures and abundant expression of the proinflammatory cytokine genes *IFNG* and *IL2* (Fig. 3, E and F). In contrast, clusters 1 and 3 overexpressed the memory-associated genes *LTB* and *IL7R,* respectively (Fig. 3E). *TNF* expression was evenly distributed among clusters, whereas *GZMB* was abundantly expressed in $CD8^+$ T cell cluster 2 and, at lower levels, in $CD8^+$ T cell cluster 4 (Fig. 3F). Each $CD8^+$ T cell cluster was also characterized by a distinct effector signature (cluster 2: *IFNG*, *CCL3*, *CCL4*, and *IL2RA*; cluster 4: *GZMA* and *CCL5*) (Fig. 3G).

Using CITE-seq, we quantified various surface markers to link the transcriptional identities of individual clusters with activation, effector, and memory phenotypes defined at the level of protein expression (Fig. 3H and fig. S5A). $CD4^+$ T cell cluster 0 (highest $CD4^+$ *IFNG* expression) was characterized by relative overexpression of several activation markers, including CD71 and PD-1, whereas $CD4^+$ T cell clusters 1 and 3 exhibited Th17-like memory ($CCR6^+CD127^+$) and memory ($CD127^+$) phenotypes, respectively. Analogously, $CD8^+$ T cell cluster 2 (highest $CD8^+$ *IFNG* expression) also exhibited relative overexpression of several activation markers, including PD-1, ICOS, HLA-DR, and CD71. Vaccination further increased the expression of PD-1 in the $CD8^+$ T cell lineage (Fig. 3I and fig. S5B), confirming our previous observations using HLA-I tetramers in conjunction with conventional flow cytometry (Fig. 2, G and H).

These results demonstrate concordant phenotypic heterogeneity at the levels of gene and protein expression and reveal the molecular landscape of spike-specific $CD4^+$ and $CD8^+$ T cells in the context of hybrid immunity against SARS-CoV-2.

IFNG upregulation is a marker of hybrid spike-specific $CD4^+$ T cell immunity

Using this combined dataset as a basis for exploration, we hypothesized that stepwise changes in gene expression from day 35 to 6–9M and from 6–9M to 18M might reflect the sequential effects of long-term memory formation and vaccination, respectively. Averaging transcript abundance across each time point and ordering gene expression by fold change revealed that cytotoxic molecules, including *GZMB* and *PRF1,* were progressively upregulated in the $CD4^+$ T cell lineage (Fig. 4A). To determine if these differences held across the spectrum of disease severity, we next performed a differential gene expression analysis of spike-specific $CD4^+$ T cells sampled on day 35 and at 6–9M and 18M after mild or severe COVID-19. Eleven genes were upregulated in all groups, including *TNF*, and other effector molecules, including *IFNG*, *GZMB,* and *PRF1*, were upregulated after vaccination in spike-specific $CD4^+$ T cells obtained from donors with a history of mild or severe COVID-19 (Fig. 4B).

In each donor group, the proportions of cells belonging to clusters 0, 1, and 3 remained stable over time (Fig. 4C). A similar pattern was observed for individual donors analyzed separately, with the exception of Dnr22, who exhibited a substantial expansion of spike-specific $CD4^+$ T cells in cluster 1 after vaccination (fig. S6A). Differential gene expression analysis further identified *CCL20*, *IFNG,* and *LGALS3* as the most highly upregulated transcripts at 18M (Fig. 4D). In addition, gene set enrichment analysis (GSEA) showed overrepresentation of the Kyoto Encyclopedia of Genes and Genomes (KEGG) ribosome pathway at 6–9M (Fig. 4E), which may be associated with an early differentiated phenotype poised for activation and effector functionality (*19*). GSEA also confirmed enrichment of *IFNG* and inflammatory response gene sets at 18M

(Fig. 4E and fig. S6B). Indeed, the proportions of cells expressing *IFNG* were elevated after vaccination in all donors with a history of mild or severe disease (Fig. 4F), but in contrast to a previous report (*17*), we found no evidence of contemporaneous increases in the frequencies of $CD4^+$ T cells expressing IL-10 (fig. S6C). Average gene expression calculations for every transcript segregated by time point further revealed that *IFNG* expression was consistently elevated at 18M, irrespective of whether clusters 0, 1, and 3 were considered together or separately (Fig. 4G).

These results indicate that spike-specific $CD4^+$ T cells shift toward a proinflammatory $IFNG^+$ phenotype after vaccination against COVID-19.

Extensive transcriptome redistribution defines hybrid spike-specific $CD8^+$ T cell immunity

SARS-CoV-2 booster vaccination increases the frequencies of spike-specific $CD8^+$ T cells to a substantially greater extent than the frequencies of spike-specific $CD4^+$ T cells, indicating greater responsiveness to recurrent antigen exposure (*20*). We therefore compared the transcriptomes of spike-specific $CD8^+$ T cells before and after vaccination. Remarkably, $CD8^+$ T cells redistributed almost entirely from cluster 4 to cluster 2 after vaccination (Fig. 5A), irrespective of initial disease severity (fig. S6D). Cluster 2, which contributed the majority of cells after vaccination, was characterized by enhanced expression of classical type 1 proinflammatory (*IFNG* and *TNF*), chemotactic (*CCL3* and *CCL4*), and inflammatory (*XCL1* and *XCL2*) chemokines/cytokines (Fig. 3G).

Using an integrated approach combining transcriptomics and TCR-seq, we attempted to identify the origins of spike-specific $CD8^+$ T cell clonotypes after vaccination. Nucleotide identity across rearranged TCRα and TCRβ sequences was used to define clonality. Spike-specific $CD8^+$ T cell clonotypes were more commonly shared between the two time points compared with $CD4^+$ T cell

clonotypes (Fig. 5B and fig. S7A) and more commonly expanded after vaccination (Fig. 5C). Most spike-specific CD8$^+$ T cell clonotypes also expressed *IFNG* at 18M (Fig. 5D). However, we found no evidence to suggest that either clonotypes recruited by the original infection or clonotypes recruited in response to subsequent vaccination preferentially expressed *IFNG* (Fig. 5D and fig. S7B), instead observing that expanded clonotypes were enriched for effector molecules (*IFNG*, *TNF*, *CCL3*, and *CCL4*) at 18M (Fig. 5E).

To further understand this dichotomy, we compared the transcriptomes of spike-specific CD8$^+$ T cell clonotypes that were present at one time point with the transcriptomes of spike-specific CD8$^+$ T cell clonotypes that were present at both time points, performing differential gene expression analysis and GSEA (fig. S8, A to C). In contrast to clonotypes that were present at both time points, which overexpressed effector genes (*XCL1*, *XCL2*, and *NKG7*), clonotypes present only at 18M overexpressed the memory-associated marker *LTB* (fig. S8A). These differences were corroborated by the enrichment of cytotoxicity and inflammatory pathways among clonotypes detected at both time points and the enrichment of IFN signaling responses among clonotypes detected only at 18M (fig. S8, B and C).

The extensive transcriptomic shift from cluster 4 to 2 raised the possibility that vaccination promoted the differentiation of spike-specific CD8$^+$ T cells initially detected at 6–9M. To test this hypothesis, we analyzed expanded clonotypes detected at 6–9M and 18M, linking cells that shared identical TCRs (Fig. 5F). Approximately half of all clonotypes from donors with a history of severe disease were present at both time points compared with only 11% of all clonotypes from donors with a history of mild disease (Fig. 5G). Interestingly, vaccination did not appear to cause a direct migration from cluster 4 (*IFNG*$^-$) to cluster 2 (*IFNG*$^+$), as only 3/41 clonotypes present at 6–9M were more commonly represented in cluster 2 at 18M (Fig. 5H).

These data suggest that vaccination increases the proportions spike-specific CD8$^+$ T cells that express *IFNG*, likely via the expansion of existing *IFNG*$^+$ cells and/or the *de novo* recruitment of *IFNG*$^+$ cells rather than via functional remodeling of *IFNG*$^-$ cells into *IFNG*$^+$ cells after induction.

Infection and vaccination timelines affect the quality and quantity of spike-specific T cells

To extend these findings, we investigated how booster vaccinations impacted spike-specific CD4$^+$ and CD8$^+$ T cells in donors with or without a prior history of infection with SARS-CoV-2. Initially, we studied a cohort of patients with chronic lymphocytic leukemia (CLL) undergoing treatment with ibrutinib, which suppresses B cell proliferation and survival by irreversibly inhibiting Bruton's tyrosine kinase (BTK), all of whom (n = 7) had received two booster vaccinations (totaling four vaccine doses) after infection with SARS-CoV-2 (fig. S9A and table S4). The frequencies of spike-specific CD8$^+$ T cells increased significantly after booster vaccination compared with baseline (fig. S9B). In contrast, the frequencies of spike-specific CD4$^+$ T cells remained largely unchanged after vaccination (fig. S9C) and approximated those observed in non-CLL donors with a history of mild or severe disease before vaccination (0.29–1.33%) (Fig. 1D), potentially reflecting a ceiling effect (*6*). These cells nonetheless showed no signs of functional exhaustion and more commonly expressed IFN-γ after vaccination (fig. S9D). Of note, the frequencies of total memory CD8$^+$ T cells expressing IFN-γ was higher in 6/7 donors after vaccination, although this trend did not reach statistical significance (fig. S9E).

We then evaluated spike-specific CD4$^+$ and CD8$^+$ T cell responses in healthy donors (n = 14) enrolled in a vaccination cohort (*21*), sampling at 3M and 18M after the second dose (Fig. 6A and table S5). At the later time point, 9/14 donors had received 3–4 doses of an mRNA vaccine without contracting SARS-CoV-2, whereas 5/14 donors had received 2–3 doses of an mRNA vaccine and experienced a breakthrough infection with SARS-CoV-2. We found no significant differences in the frequencies of spike-specific CD4$^+$ or CD8$^+$ T cells at 3M versus 18M (Fig. 6, B and C) or the

proportions of cytokine-producing $CD4^+$ or $CD8^+$ T cells associated with breakthrough infection (Fig. 6, D and E) or vaccination alone (Fig. 6, F and G). Increased frequencies of IFN-γ^+ $CD8^+$ T cells were nonetheless observed in the contexts of breakthrough infection (Fig. 6E) and vaccination alone (Fig. 6G), albeit without achieving statistical significance.

These findings show that booster vaccination after infection can augment the frequencies and functional qualities of spike-specific $CD4^+$ and $CD8^+$ T cells in the circulation, whereas booster vaccination in the absence of prior infection does not significantly enhance the frequencies and functional qualities of spike-specific $CD4^+$ and $CD8^+$ T cells in the circulation (fig. S10).

DISCUSSION

SARS-CoV-2 vaccination has saved tens of millions of lives during the current pandemic by reducing the incidence of severe COVID-19 (*22*). In particular, durable protection from severe disease has been observed in patients with hybrid immunity (*5*), indicating that long-term immunological memory could play a key role. In this study, we assessed the frequencies and functional qualities of SARS-CoV-2-specific $CD4^+$ and $CD8^+$ T cells in donors with a history of mild or severe disease before and after mRNA vaccination. We found that non-spike-specific $CD4^+$ T cells retained their original functional characteristics but declined numerically over time. In contrast, the frequencies and functional capabilities of spike-specific $CD4^+$ and $CD8^+$ T cells increased after vaccination, despite the upregulation of inhibitory receptors among spike-specific $CD8^+$ T cells compared with baseline. Booster vaccination also enhanced the functional profiles of spike-specific $CD4^+$ T cells and the frequencies of spike-specific $CD8^+$ T cells in previously infected patients with CLL. However, no such changes were observed in previously vaccinated but uninfected individuals after boosting or breakthrough infection, suggesting that recurrent antigen exposure in this context may simply counteract waning immunity (*23, 24*). These collective findings demonstrate that vaccination can enhance T cell immunity without necessarily inducing T cell exhaustion after infection with SARS-CoV-2.

T cells often upregulate multiple inhibitory receptors in response to severe COVID-19 (*25*). This phenomenon has been associated with functional exhaustion in the context of chronic viral infections, such as HIV-1 (*26*), and likely reflects an immunological adaptation to ongoing antigen exposure (*27*). However, inhibitory receptor expression during early infection with SARS-CoV-2 may simply demarcate *de novo* virus-specific T cell activation (*28*), especially given the high levels of viral replication that accompany severe disease (*29*). Our data align with this notion. We also found that spike-specific and nucleocapsid-specific $CD4^+$ T cells were more polyfunctional after severe versus mild COVID-19. Moreover, vaccination enhanced the functional profiles of spike-

specific CD4+ and CD8+ T cells in donors with a history of severe disease and further increased inhibitory receptor expression among spike-specific CD8+ T cells, consistent with robust immunological memory rather than exhaustion. These observations suggest that vaccination may help protect convalescent individuals recovering from severe disease against future encounters with SARS-CoV-2.

SARS-CoV-2 vaccination has been associated with dysfunctional T cell immunity (*30, 31*). To assess this possibility in more detail, we used *ex vivo* peptide stimulation in conjunction with flow cytometry and scRNA-seq to profile SARS-CoV-2-specific CD4+ and CD8+ T cells functionally, phenotypically, and transcriptomically. We found that spike-specific CD4+ and CD8+ T cells overexpressed many proinflammatory chemokines and cytokines after vaccination, including IFN-γ. These data align with previous work showing that mRNA vaccination induces strong inflammatory responses (*32*) and potentially drives spike-specific CD4+ T cell clonotypes into a T_H1-like differentiation program (*33*). However, we did not identify spike-specific CD4+ T cells coexpressing IFN-γ and IL-10, which could potentially balance inflammatory signals in the context of hybrid immunity (*17*). Of note, the scRNA-seq data indicated distinct transcriptional remodeling of the CD4+ and CD8+ T cell lineages after vaccination. In particular, the overall memory response was altered among spike-specific CD4+ T cells and skewed toward greater cytokine production (*e.g.*, *IFNG* and *TNF*), without necessarily affecting T_H1-like chemokine receptor expression patterns (*e.g.*, *CXCR3*) or cluster identity. In contrast, spike-specific CD8+ T cells underwent a marked transcriptional shift toward an *IFNG*+ response profile, feasibly enabling anamnestic responses characterized by the rapid production of IFN-γ. We also found that the *IFNG* phenotype among spike-specific CD8+ T cells was tightly linked with the expression of distinct TCRs. Accordingly, vaccination likely expands the relative frequencies of existing *IFNG*+ clonotypes and/or preferentially recruits new *IFNG*+ clonotypes, although we were unable to distinguish

between these possibilities by definitively identifying the origins of emerging *IFNG*$^+$ clonotypes at 18M.

T cell responses that simultaneously deliver multiple antiviral effector functions have been associated with clearance or enhanced immune control of many viral infections, but coexpression of IL-10 can limit immunopathology (*34, 35*) and has been associated with asymptomatic COVID-19 (*36*). We found that IFN-γ expression induced by mRNA vaccination was a hallmark of hybrid immunity. IFN-γ exhibits potent antiviral effects and has been used successfully to treat immunocompromised patients infected with SARS-CoV-2 (*37*). In addition, low serum levels of IFN-γ, together with advanced age and a lack of vaccination, have been associated independently with the risk of contracting severe COVID-19 (*38*). CD8$^+$ T cells are major producers of IFN-γ. This cytokine suppresses viral replication via the upregulation of interferon-stimulated genes (ISGs), which enhance antigen presentation and recruit multiple immune cell types to the site of infection (*39*). Moreover, recent data indicate that mRNA vaccination induces protection in B cell-deficient mice, attributable to T cell immunity via the production of IFN-γ (*40*). Enhanced T cell effector functionality with a balanced inflammatory profile in the setting of hybrid immunity could therefore mediate durable protection against severe COVID-19.

There are several limitations to our study. First, all donors with a history of mild or severe disease were infected with and vaccinated against the Wuhan strain of SARS-CoV-2, which allowed us to track immune responses specific for a defined antigen over time but nonetheless excluded similar analyses of individuals infected with more recent variants and/or vaccinated with booster formulations against subvariants of Omicron. However, this is likely a minor consideration, given that ancestral T cells efficiently cross-recognize the Omicron variant of SARS-CoV-2 (*41–43*). Second, we did not actively match individuals with a history mild or severe disease for comorbidities, potentially confounding associations between the nature of the immune response

and the initial severity of COVID-19. Third, our recently vaccinated donor harbored a small population of spike-specific $CD8^+$ T cells before and after vaccination, precluding the possibility of tracking individual clonotypes to discriminate between anamnestic and *de novo* clonal expansions over time. Fourth, our scRNA-seq experiments were potentially confounded by gender bias, given that all three donors with a history of mild disease were male, whereas just one donor with a history of severe disease was male. Fifth, limited cell numbers were available for scRNA-seq, limiting our ability to discern the origins of newly detected *IFNG*$^+$ spike-specific $CD8^+$ T cell clonotypes after infection or subsequent vaccination.

In summary, we have shown that spike-specific but not non-spike specific $CD4^+$ and $CD8^+$ T cells become more polyfunctional in previously infected individuals after mRNA vaccination, irrespective of inhibitory receptor expression and the initial severity of COVID-19. We have also demonstrated that upregulated expression of IFN-γ among spike-specific $CD4^+$ and $CD8^+$ T cell clonotypes is a common hallmark of vaccine-induced hybrid immunity. Collectively, these data indicate that vaccination after infection is associated with cumulative immunological benefits over time, potentially conferring enhanced protection against subsequent exposure to SARS-CoV-2.

MATERIALS AND METHODS

Study design

SARS-CoV-2-specific T cell responses in convalescent donors were evaluated via flow cytometry and scRNA-seq after natural infection and after subsequent mRNA vaccination. Equivalent analyses were performed to assess the impact of altered B cell functionality in patients undergoing treatment with a BTK inhibitor for CLL and to calibrate the data as a function of multiple vaccinations in relation to infection with SARS-CoV-2.

Patient samples

Venous blood samples were obtained from convalescent donors after infection with SARS-CoV-2, confirmed via RT-PCR testing at the Karolinska University Hospital, Stockholm, Sweden. Disease severity was stratified as mild or severe based on hospitalization for COVID-19 (table S1). All donors were infected during the first wave of SARS-CoV-2, peaking in March and April 2020. Samples were collected 6–9 months after COVID-19 (6–9M) and/or 18 months after COVID-19 (18M). Participants were vaccinated primarily with mRNA formulations offered by The Public Health Agency of Sweden. Additional venous blood samples were obtained from convalescent donors on day 35 after symptom onset (n = 3) and from patients undergoing treatment with ibrutinib for CLL (n = 7). The latter were sampled after natural infection and after a fourth vaccine dose (table S4). Six of these donors were hospitalized with COVID-19. A further donor with previously confirmed infection was sampled 2 weeks before and 2 weeks after double vaccination. Healthy vaccinated controls (n = 14) were recruited via the COVAXID Study (*21*) as detailed in table S5. PBMCs were isolated via standard density gradient centrifugation and cryopreserved in fetal bovine serum (FBS) containing 10% dimethyl sulfoxide (DMSO). Written informed consent was obtained from all donors in accordance with the principles of the

Declaration of Helsinki. The study was approved by the Swedish Ethical Review Authority and by regional ethics boards at the University of California, San Diego, USA.

Peptides

Surface markers were analyzed after stimulation with peptide pools (15mers overlapping by 11 amino acids) spanning the entire spike protein of SARS-CoV-2 (Peptides&Elephants GmbH). Functional analyses of $CD4^+$ T cells via the identification of intracellular markers were performed after stimulation with peptide pools (20mers overlapping by 10 amino acids) spanning the entire spike, nucleocapsid, combined membrane and envelope, and combined ORF3–10 proteins of SARS-CoV-2 (Sigma-Aldrich). AIM expression among unstimulated $CD8^+$ T cells was prohibitively high after staining intracellularly. Functional analyses of $CD8^+$ T cells via the identification of intracellular markers were therefore performed using a pool of HLA-I-restricted and HLA-II-restricted peptides representing immunodominant epitopes from the spike protein of SARS-CoV-2 (Sigma-Aldrich) and limited to the detection of IFN-γ. All peptide sequences were based on the ancestral Wuhan strain of SARS-CoV-2. Lyophilized peptides were reconstituted at a stock concentration of 10 mg/ml in DMSO and diluted to 100 µg/ml in phosphate-buffered saline (PBS).

Activation-induced marker assay

PBMCs were thawed quickly, resuspended in complete medium in the presence of DNase I (10 U/ml, Sigma-Aldrich), and rested at 1×10^6 cells/well in 96-well U-bottom plates (Corning) for 3 h at 37°C. For surface analyses, the medium was supplemented with anti-CXCR5–BB515 (clone RF8B2, BD Biosciences) and unconjugated anti-CD40 (clone HB14, Miltenyi Biotec), followed 15 min later by the relevant peptides (each at 0.5 µg/ml). Cells were then incubated for 12 h at 37°C. For intracellular analyses, the medium was supplemented with anti-CXCR5–BB515 (clone RF8B2, BD Biosciences), followed 15 min later by the relevant peptides (each at 0.5 µg/ml) and a further 1 h later by brefeldin A (1 µg/ml, Sigma-Aldrich) and monensin (0.7 µg/ml, BD

Biosciences). Cells were then incubated for 9 h at 37°C. Negative control wells lacked peptides and contained volume-equivalent DMSO.

Flow cytometry

Cells were stimulated as described above, washed in FACS buffer (PBS supplemented with 2% FBS and 2 mM EDTA), and stained as detailed in tables S6 and S7. Stained cells were then fixed with 1% paraformaldehyde in PBS and acquired using a FACSymphony A5 (BD Biosciences). Data were analyzed using FlowJo version 10 (FlowJo LLC). Healthy vaccinated controls were evaluated using a reduced surface panel, excluding CCR4, CCR6, and CXCR3 from table S6, and a reduced surface and intracellular panel, excluding CCR4, CCR6, CXCR3, CD38, and PD-1 from table S7. Stimulation indices were calculated by dividing the frequencies of AIM^+ cells in experimental wells containing the relevant peptides by the corresponding frequencies of AIM^+ cells in negative control wells containing volume-equivalent DMSO. Analyses of intracellular AIM^+ $CD4^+$ T cells or IFN-γ^+ $CD8^+$ T cells were limited to populations with a minimum of 10 events in the corresponding target gate. Functional profiles were compared using a permutation test and visualized in SPICE version 6 (https://niaid.github.io/spice/).

Tetramers

HLA-I tetramers were generated as described previously (*44*). The following specificities were used in this study: SARS-CoV-2 spike A*0201 YLQPRTFLL, SARS-CoV-2 spike A*2402 QYIKWPWYI, SARS-CoV-2 spike B*0702 SPRRARSVA, SARS-CoV-2 nucleocapsid A*0201 LLLDRLNQL, SARS-CoV-2 nucleocapsid B*0702 SPRWYFYYL, SARS-CoV-2 ORF3a A*0201 LLYDANYFL, SARS-CoV-2 ORF3a A*0201 ALSKGVHFV, CMV pp65 A*0201 NLVPMVATV, and CMV pp65 B*0702 TPRVTGGGAM. Donors were typed via flow cytometry using anti-HLA-A2–PE-Cy7 (clone BB7.2, BioLegend), anti-HLA-A24–FITC (clone 220, MBL International), and anti-HLA-B7–APC (clone BB7.1 BioLegend). The relevant tetramers were then used in conjunction

with a panel of surface markers to identify and phenotype virus-specific $CD8^+$ T cells as detailed in table S8.

Single-cell RNA sequencing

PBMCs were stimulated with spike peptides as described above and stained as detailed in table S9. Stained cells were then sorted as lymphocytes/singlets/viable/$CD4^+$/$CD69^+CD40L^+$ or lymphocytes/singlets/viable/$CD8^+$/$CD69^+$4-1BB$^+$ populations using an MA900 Multi-Application Cell Sorter (Sony Biotechnology). Cells stained with unique hashing antibodies were sorted from up to three samples into a single microfuge tube (Sarstedt). Pooled samples were loaded onto a Chromium Single Cell Chip (10x Genomics). Libraries were prepared using a Chromium Next GEM Single Cell V(D)J Reagent Kit v1.1 (10x Genomics). Sequencing was performed using an 8-base index read, a 26-base read 1 containing barcodes and unique molecular identifiers (UMIs), and a 98-base read 2 containing transcript sequences to a depth of approximately 50,000 to 90,000 reads per cellular barcode on a NovaSeq6000 SP100 Flow Cell (Illumina).

Single-cell RNA analysis

Sequencing outputs were delivered as demultiplexed fastq files and processed into expression matrices using the multi command in CellRanger version 6.1.1 (10x Genomics). Expression data (gene, protein, and hashtag) were imported using the Read10X function in Seurat version 4.1.1 (*45*). Cell inclusion required fewer than 6% of reads aligned to mitochondrial genes and a distinct gene expression range from 1000 to 5700. Transcript expression was normalized using the LogNormalize option from the NormalizeData function in Seurat version 4.1.1. Antibody and hashtag data were transformed using the centered log-ratio approach. Hashtag oligo (HTO) demultiplexing was performed using the HTODemux function in Seurat version 4.1.1. Antibody detection was used to group cells according to the expression of CD4 or CD8. TCR data were imported using the import_vdj command in the djvdj package in R and filtered to retain only the

most commonly expressed α and β chain sequences, grouping cells as a single clonotype if these sequences matched exactly. Alluvial plots for shared clonotypes between time points were generated for the top 50 sequences using the compareClonotypes function in scRepertoire version 1.4.0 (*46*). Data from additional samples processed in distinct batches were integrated using the SelectIntegrationFeatures, FindIntegrationAnchors, and IntegrateData functions in Seurat version 4.1.1. Cells were clustered using the FindNeighbors function with the first 20 principal component dimensions and a resolution of 0.2 for the FindClusters function in Seurat version 4.1.1. Dimensionality reduction was performed using UMAP. Irrelevant cells expressing CD8 were eliminated from the analysis by removing NK cells (UMAP cluster 5), MAIT cells (UMAP cluster 6), γδ T cells (expressing *TRGV3*, *TRGV9, TRDV1*, or *TRDV3*), and NKT cells (coexpressing *TRAV10* and *TRAJ18*). GSEA was performed using the fgsea package in R with 5000 permutations and gene sets downloaded from the MSigDB. Differential gene expression analyses were performed using the FindMarkers and FindAllMarkers functions with the Wilcoxon rank-sum test in Seurat version 4.1.1. Average gene expression was calculated using the AverageExpression function in Seurat version 4.1.1. Figures were prepared using ggplot2 and Seurat version 4.1.1 in R.

Statistics

Statistical analyses were performed using Prism software version 9 (GraphPad) and R version 4.1.3. Paired samples were compared using the Wilcoxon signed-rank test, and unpaired samples were compared using the Mann-Whitney U test. In all dot plots, horizontal bars represent median values, and in all figures, significance is denoted as follows: n.s. (not significant), $*P < 0.05$, $**P < 0.01$, $***P < 0.001$, $****P < 0.0001$.

ACKNOWLEDGMENTS

We express our gratitude to all donors, healthcare personnel, study coordinators, administrators, and laboratory managers involved in this work. The authors acknowledge support from the National Genomics Infrastructure in Stockholm funded by the SciLifeLab, the Knut and Alice Wallenberg Foundation, and the Swedish Research Council, and from the SNIC/Uppsala Multidisciplinary Center for Advanced Computational Science for assistance with massively parallel sequencing and access to the UPPMAX computational infrastructure. This study was funded by grants from the SciLifeLab National COVID-19 Research Program, the CIMED Grant Program at the Karolinksa Institutet, the Knut and Alice Wallenberg Foundation, and the Swedish Research Council. C.C. was supported by the Karolinska Institutet (2022-01708). Y.G. was supported by the Karolinska Institutet (2022-01968). D.A.P. was supported by the National Institute for Health Research (COV-LT2-0041). M.B. was supported by the Swedish Research Council (2018-02330, 2020-06121, and 2021-04779), the Knut and Alice Wallenberg Foundation (KAW 2021.0136), the European Research Council (101057129 and 101041484), the Karolinska Institutet (2019-00969), the Swedish Society for Medical Research (CG-22-0009), the Swedish Cancer Society (22 2237 Pj), the Åke Wibergs Stiftelse (M20-0190), and the Jonas Söderquist Stiftelse.

AUTHOR CONTRIBUTIONS

Conceptualization: C.C., Y.G., S.Al., and M.B. Methodology: C.C., Y.G., S.Ad., and O.R.B. Analysis: C.C., Y.G., and S.Ad. Visualization: C.C., Y.G., and S.Ad. Sample collection and resources: L.H., A.Ö., P.B., H.-G.L., N.B., K.S., S.L.-L., D.A.P., C.Q., A.G., D.W., E.J.W., A.S., S.Al., and M.B. Funding acquisition: A.Ö., J.K.S., D.A.P., C.Q., S.Al., and M.B. Supervision: A.Ö., J.K.S., D.A.P., C.Q., A.G., D.W., E.J.W., A.S., S.Al., and M.B. Writing (original draft): C.C. and M.B. Writing (review & editing): C.C., Y.G., D.A.P., and M.B. All authors contributed intellectually and approved the final version of the manuscript for publication.

COMPETING INTERESTS

E.J.W. is a member of the Parker Institute for Cancer Immunotherapy, which supported this study. E.J.W. is an advisor for Danger Bio, Janssen, New Limit, Marengo, Pluto Immunotherapeutics, Related Sciences, Santa Ana Bio, Synthekine, and Surface Oncology. E.J.W. is a founder of and holds stock in Surface Oncology, Danger Bio, and Arsenal Biosciences. A.S. is a consultant for Gritstone Bio, Flow Pharma, Moderna, AstraZeneca, Qiagen, Fortress, Gilead, Sanofi, Merck, RiverVest, MedaCorp, Turnstone, NAVaccine Institute, Emervax, Gerson Lehrman Group, and Guggenheim. S.Al. has received honoraria for lectures and educational events from Gilead, AbbVie, MSD, and Biogen and reports grants from Gilead and AbbVie. M.B. is a consultant for Oxford Immunotec, Mabtech, BMS, and MSD. All other authors declare that they have no competing interests.

DATA AVAILABILITY

Expression matrices from single-cell sequencing experiments have been deposited in ArrayExpress under the accession number E-MTAB-12716. Requests for other data should be addressed to the corresponding authors, Curtis Cai and Marcus Buggert.

CODE AVAILABILITY

R codes for single-cell analyses are available via Zenodo (https://doi.org/10.5281/zenodo.7594134).

FIGURE LEGENDS

Figure 1. Frequencies of SARS-CoV-2-specific T cells after infection and vaccination. (**A**) Overview of the experimental design. (**B**) Time between vaccination and sampling at 18M. Data are shown for donors with matched samples at 6–9M and 18M. (**C**) Representative flow cytometry plots showing the identification of spike-specific $CD4^+$ T cells via activation-induced marker (AIM) expression. (**D**) Frequencies of AIM^+ memory $CD4^+$ T cells targeting different regions of SARS-CoV-2. (**E**) Comparison of AIM^+ memory $CD4^+$ T cell frequencies at 6–9 versus 18M. (**F**) Representative flow cytometry plots showing the identification of spike-specific $CD8^+$ T cells via AIM expression. (**G**) Comparison of AIM^+ memory $CD8^+$ T cell frequencies in donors grouped by time point and disease severity.

Figure 2. Functionality and inhibitory receptor expression among SARS-CoV-2 spike-specific T cells after infection and vaccination. (**A**) Representative flow cytometry plots showing cytokine expression among AIM^+ memory $CD4^+$ T cells. (**B**) Percentages of AIM^+ memory $CD4^+$ T cells with cytokine expression. (**C**) SPICE analysis of cytokine expression among SARS-CoV-2-specific memory $CD4^+$ T cells. (**D**) Representative flow cytometry plots showing cytokine and cytotoxic molecule expression among spike-specific memory $CD8^+$ T cells after peptide stimulation. (**E**) Percentages of IFN-γ^+ spike-specific and total memory $CD8^+$ T cells with polyfunctional cytokine and cytotoxic molecule expression after peptide stimulation. (**F**) Representative flow cytometry plots showing the identification of tetramer-binding $CD8^+$ T cells specific for SARS-CoV-2 spike or CMV epitopes. (**G**) Representative flow cytometry histograms showing PD-1 or TIM3 expression among spike-specific $CD8^+$ T cells. (**H**) Percentages of tetramer-binding $CD8^+$ T cells with PD-1 or TIM3 expression.

Figure 3. Single-cell analysis of SARS-CoV-2 spike-specific T cells after infection and vaccination. (**A**) Overview of donors and sampling time points selected for scRNA-seq. (**B**) UMAP and clustering of sorted AIM$^+$ CD4$^+$ and CD8$^+$ T cells responding to spike peptide stimulation. (**C**) Expression of CD4 and CD8 at the protein and transcript levels. (**D**) Distribution of conventional AIM$^+$ CD4$^+$ and CD8$^+$ T cells from each donor group. (**E**) Dot plot showing differentially expressed genes in the CD4$^+$ T cell clusters. (**F**) Violin plots showing the expression of selected markers previously measured via flow cytometry. (**G**) Dot plot showing differentially expressed genes in the CD8$^+$ T cell clusters. (**H**) Heatmap showing protein expression measured via CITE-seq. (**I**) Violin plots showing the expression of activation markers separated by time point.

Figure 4. SARS-CoV-2 spike-specific CD4$^+$ T cells exhibit a proinflammatory profile in the setting of hybrid immunity. (**A**) Ranked comparison of average transcription expression in AIM$^+$ CD4$^+$ T cells grouped by time point. (**B**) Venn diagram showing differentially expressed genes shared among groups compared with AIM$^+$ CD4$^+$ T cells from recently infected donors sampled on day 35. (**C**) Proportions of AIM$^+$ CD4$^+$ T cells belonging to each CD4$^+$ T cell cluster. (**D**) Volcano plot showing differentially expressed genes between AIM$^+$ CD4$^+$ T cells at 6–9M versus 18M. (**E**) Gene set enrichment analysis of differentially expressed genes between AIM$^+$ CD4$^+$ T cells at 6–9M versus 18M showing significant hits from the KEGG and Hallmark pathways. (**F**) Percentages of AIM$^+$ CD4$^+$ T cells with expression of *IFNG*. (**G**) Comparison of average gene expression for all AIM$^+$ CD4$^+$ T cells versus individual CD4$^+$ T cell clusters separated by time point. Labels identify the top six genes with the largest differences in expression.

Figure 5. SARS-CoV-2 spike-specific CD8$^+$ T cells shift to a proinflammatory phenotype via clonal recruitment or expansion after vaccination in the setting of hybrid immunity. (**A**) Proportions of AIM$^+$ CD8$^+$ T cells belonging to each CD8$^+$ T cell cluster. (**B**) Proportions of AIM$^+$

CD8$^+$ T cells with paired TCRα and TCRβ chain sequences detected only at 18M or at 6–9M and at 18M. (**C**) Alluvial plots showing shared AIM$^+$ CD8$^+$ T cell clonotypes before and after vaccination. (**D**) *IFNG* expression among expanded AIM$^+$ CD8$^+$ T cell clonotypes after vaccination. (**E**) Volcano plot showing differentially expressed genes between clonally expanded AIM$^+$ CD8$^+$ T cells at 6–9M versus 18M. (**F**) UMAP plot of clonally expanded AIM$^+$ CD8$^+$ T cells. Lines connect shared clonotypes. (**G**) Comparison of expanded AIM$^+$ CD8$^+$ T cell clonotypes from all time points showing fractional representation at 6–9M. The percentages of AIM$^+$ CD8$^+$ T cell clonotypes detected at both time points are shown above. (**H**) Fractional representation of AIM$^+$ CD8$^+$ T cell clonotypes present at both time points in cluster 4. Lines connect identical clonotypes.

Figure 6. SARS-CoV-2 spike-specific T cells are minimally impacted by breakthrough infection or booster vaccination. (**A**) Overview of healthy vaccinated donors and sampling time points. (**B**) Frequencies of AIM$^+$ memory CD4$^+$ T cells in healthy vaccinated donors. (**C**) Frequencies of AIM$^+$ memory CD8$^+$ T cells in healthy vaccinated donors. (**D**) Percentages of AIM$^+$ memory CD4$^+$ T cells expressing cytokines after breakthrough infection. (**E**) Percentages of total memory and IFN-γ$^+$ memory CD8$^+$ T cells expressing cytokines and cytotoxic molecules after breakthrough infection. (**F**) Percentages of AIM$^+$ memory CD4$^+$ T cells expressing cytokines after vaccination. (**G**) Percentages of AIM$^+$ memory CD8$^+$ T cells expressing cytokines and cytotoxic molecules after vaccination.

SUPPLEMENTARY MATERIALS

REFERENCES

1. A. A. Quadeer, S. F. Ahmed, M. R. McKay, Landscape of epitopes targeted by T cells in 852 individuals recovered from COVID-19: meta-analysis, immunoprevalence, and web platform. *Cell Rep Med* **2**, 100312 (2021).
2. A. A. Minervina *et al.*, SARS-CoV-2 antigen exposure history shapes phenotypes and specificity of memory CD8$^+$ T cells. *Nat Immunol* **23**, 781–790 (2022).
3. S. Gazit *et al.*, The incidence of SARS-CoV-2 reinfection in persons with naturally acquired immunity with and without subsequent receipt of a single dose of BNT162b2 vaccine: a retrospective cohort study. *Ann Intern Med* **175**, 674–681 (2022).
4. P. Nordstrom, M. Ballin, A. Nordstrom, Risk of SARS-CoV-2 reinfection and COVID-19 hospitalisation in individuals with natural and hybrid immunity: a retrospective, total population cohort study in Sweden. *Lancet Infect Dis* **22**, 781–790 (2022).
5. N. Bobrovitz *et al.*, Protective effectiveness of previous SARS-CoV-2 infection and hybrid immunity against the omicron variant and severe disease: a systematic review and meta-regression. *Lancet Infect Dis* **23**, 556–567 (2023).
6. A. P. S. Munro *et al.*, Safety, immunogenicity, and reactogenicity of BNT162b2 and mRNA-1273 COVID-19 vaccines given as fourth-dose boosters following two doses of ChAdOx1 nCoV-19 or BNT162b2 and a third dose of BNT162b2 (COV-BOOST): a multicentre, blinded, phase 2, randomised trial. *Lancet Infect Dis* **22**, 1131–1141 (2022).
7. M. M. Painter *et al.*, Rapid induction of antigen-specific CD4$^+$ T cells is associated with coordinated humoral and cellular immunity to SARS-CoV-2 mRNA vaccination. *Immunity* **54**, 2133–2142.e3 (2021).
8. K. M. Wragg *et al.*, Establishment and recall of SARS-CoV-2 spike epitope-specific CD4$^+$ T cell memory. *Nat Immunol* **23**, 768–780 (2022).
9. B. Diao *et al.*, Reduction and functional exhaustion of T cells in patients with coronavirus disease 2019 (COVID-19). *Front Immunol* **11**, 827 (2020).
10. J. Neidleman *et al.*, Distinctive features of SARS-CoV-2-specific T cells predict recovery from severe COVID-19. *Cell Rep* **36**, 109414 (2021).
11. S. Kreutmair *et al.*, Distinct immunological signatures discriminate severe COVID-19 from non-SARS-CoV-2-driven critical pneumonia. *Immunity* **54**, 1578–1593.e5 (2021).
12. S. Shahbaz *et al.*, The quality of SARS-CoV-2-specific T cell functions differs in patients with mild/moderate versus severe disease, and T cells expressing coinhibitory receptors are highly activated. *J Immunol* **207**, 1099–1111 (2021).
13. A. J. Wilk *et al.*, A single-cell atlas of the peripheral immune response in patients with severe COVID-19. *Nat Med* **26**, 1070–1076 (2020).
14. A. Kusnadi *et al.*, Severely ill COVID-19 patients display impaired exhaustion features in SARS-CoV-2-reactive CD8$^+$ T cells. *Sci Immunol* **6**, eabe4782 (2021).
15. Y. Gao *et al.*, Immunodeficiency syndromes differentially impact the functional profile of SARS-CoV-2-specific T cells elicited by mRNA vaccination. *Immunity* **55**, 1732–1746.e5 (2022).
16. R. R. Goel *et al.*, mRNA vaccines induce durable immune memory to SARS-CoV-2 and variants of concern. *Science* **374**, abm0829 (2021).
17. L. B. Rodda *et al.*, Imprinted SARS-CoV-2-specific memory lymphocytes define hybrid immunity. *Cell* **185**, 1588–1601.e14 (2022).
18. E. J. Wherry, T cell exhaustion. *Nat Immunol* **12**, 492–499 (2011).
19. S. Ricciardi *et al.*, The translational machinery of human CD4$^+$ T cells is poised for activation and controls the switch from quiescence to metabolic remodeling. *Cell Metab* **28**, 895–906.e5 (2018).
20. R. L. Atmar *et al.*, Homologous and heterologous Covid-19 booster vaccinations. *N Engl J Med* **386**, 1046–1057 (2022).
21. P. Bergman *et al.*, Safety and efficacy of the mRNA BNT162b2 vaccine against SARS-CoV-2 in five groups of immunocompromised patients and healthy controls in a prospective open-label clinical trial. *EBioMedicine* **74**, 103705 (2021).
22. O. J. Watson *et al.*, Global impact of the first year of COVID-19 vaccination: a mathematical modelling study. *Lancet Infect Dis* **22**, 1293–1302 (2022).
23. Z. Zhang *et al.*, Humoral and cellular immune memory to four COVID-19 vaccines. *Cell* **185**, 2434–2451.e17 (2022).

24. G. Guerrera *et al.*, BNT162b2 vaccination induces durable SARS-CoV-2-specific T cells with a stem cell memory phenotype. *Sci Immunol* **6**, eabl5344 (2021).
25. J. Niessl, T. Sekine, M. Buggert, T cell immunity to SARS-CoV-2. *Semin Immunol* **55**, 101505 (2021).
26. M. Buggert *et al.*, T-bet and Eomes are differentially linked to the exhausted phenotype of $CD8^+$ T cells in HIV infection. *PLoS Pathog* **10**, e1004251 (2014).
27. L. M. McLane, M. S. Abdel-Hakeem, E. J. Wherry, CD8 T cell exhaustion during chronic viral infection and cancer. *Annu Rev Immunol* **37**, 457–495 (2019).
28. T. Sekine *et al.*, Robust T cell immunity in convalescent individuals with asymptomatic or mild COVID-19. *Cell* **183**, 158–168.e14 (2020).
29. O. Puhach, B. Meyer, I. Eckerle, SARS-CoV-2 viral load and shedding kinetics. *Nat Rev Microbiol* **21**, 147–161 (2023).
30. P. Chevaisrakul *et al.*, Hybrid and herd immunity 6 months after SARS-CoV-2 exposure among individuals from a community treatment program. *Sci Rep* **13**, 763 (2023).
31. J. D. Benitez Fuentes *et al.*, Evidence of exhausted lymphocytes after the third anti-SARS-CoV-2 vaccine dose in cancer patients. *Front Oncol* **12**, 975980 (2022).
32. J. R. Teijaro, D. L. Farber, COVID-19 vaccines: modes of immune activation and future challenges. *Nat Rev Immunol* **21**, 195–197 (2021).
33. U. Sahin *et al.*, COVID-19 vaccine BNT162b1 elicits human antibody and T_H1 T cell responses. *Nature* **586**, 594–599 (2020).
34. J. Sun, R. Madan, C. L. Karp, T. J. Braciale, Effector T cells control lung inflammation during acute influenza virus infection by producing IL-10. *Nat Med* **15**, 277–284 (2009).
35. J. Zhao *et al.*, Airway memory $CD4^+$ T cells mediate protective immunity against emerging respiratory coronaviruses. *Immunity* **44**, 1379–1391 (2016).
36. N. Le Bert *et al.*, Highly functional virus-specific cellular immune response in asymptomatic SARS-CoV-2 infection. *J Exp Med* **218**, e20202617 (2021).
37. A. van Laarhoven *et al.*, Interferon gamma immunotherapy in five critically ill COVID-19 patients with impaired cellular immunity: a case series. *Med* **2**, 1163–1170.e2 (2021).
38. M. Cremoni *et al.*, Low baseline IFN-γ response could predict hospitalization in COVID-19 patients. *Front Immunol* **13**, 953502 (2022).
39. M. Y. Bhat *et al.*, Comprehensive network map of interferon gamma signaling. *J Cell Commun Signal* **12**, 745–751 (2018).
40. X. Wang *et al.*, Vaccine-induced protection against SARS-CoV-2 requires IFN-γ-driven cellular immune response. *Nat Commun* **14**, 3440 (2023).
41. Y. Gao *et al.*, Ancestral SARS-CoV-2-specific T cells cross-recognize the Omicron variant. *Nat Med* **28**, 472–476 (2022).
42. A. Tarke *et al.*, SARS-CoV-2 vaccination induces immunological T cell memory able to cross-recognize variants from Alpha to Omicron. *Cell* **185**, 847–859.e11 (2022).
43. C. H. GeurtsvanKessel *et al.*, Divergent SARS-CoV-2 Omicron-reactive T and B cell responses in COVID-19 vaccine recipients. *Sci Immunol* **7**, eabo2202 (2022).
44. D. A. Price *et al.*, Avidity for antigen shapes clonal dominance in $CD8^+$ T cell populations specific for persistent DNA viruses. *J Exp Med* **202**, 1349–1361 (2005).
45. Y. Hao *et al.*, Integrated analysis of multimodal single-cell data. *Cell* **184**, 3573–3587.e29 (2021).
46. N. Borcherding, N. L. Bormann, G. Kraus, scRepertoire: an R-based toolkit for single-cell immune receptor analysis. *F1000Res* **9**, 47 (2020).

SUPPLEMENTARY FIGURE LEGENDS

Figure S1. Detection of AIM$^+$ T cells. (**A**) Representative flow cytometric gating strategy showing the identification of AIM$^+$ memory CD4$^+$ and CD8$^+$ T cells via flow cytometry. (**B**) Stimulation indices of individual donor responses at 6–9M.

Figure S2. Effect of vaccination on the frequencies of spike-specific T cells. (**A**) Frequencies of AIM$^+$ memory CD4$^+$ T cells targeting different regions of SARS-CoV-2. (**B**) Frequencies of AIM$^+$ memory CD8$^+$ T cells targeting the spike protein of SARS-CoV-2.

Figure S3. Characterization of T cell cytokine production and inhibitory receptor expression. (**A**) Permutation test comparisons of cytokine expression profiles among AIM$^+$ memory CD4$^+$ T cells (related to Fig. 2C). (**B**) Percentages of IFN-γ$^+$ spike-specific memory CD8$^+$ T cells with polyfunctional cytokine and cytotoxic molecule expression after peptide stimulation. (**C**) Representative flow cytometry plots showing the identification of inhibitory receptor expression among tetramer-binding CD8$^+$ T cells. (**D**) Percentages of tetramer-binding CD8$^+$ T cells with inhibitory receptor expression.

Figure S4. Classification of AIM$^+$ T cell populations sorted for scRNA-seq. (**A**) Representative flow cytometric gating strategy for the identification and sorting of AIM$^+$ CD4$^+$ and CD8$^+$ T cells for scRNA-seq. (**B**) Distribution of conventional AIM$^+$ cells with CD4 or CD8 protein expression separated by donor and time point. Cells classified as “other” either lacked expression of CD4 and CD8 or expressed both CD4 and CD8. (**C**) UMAP and clustering of all sorted cells, including NK cells and unconventional T cells. (**D**) Classification of NK cells and unconventional T cells. (**E**) Expression of transcripts corresponding to conventional and unconventional T cell subsets. (**F**) Distribution of donor groups and time points across each UMAP cluster. (**G**) Frequencies of sorted AIM$^+$ memory CD4$^+$ and CD8$^+$ T cells determined via flow cytometry. Time points 1 and 2 correspond to pre-vaccination and post-vaccination, respectively.

Figure S5. Protein expression among spike-specific T cells determined via CITE-seq. (**A**) Heatmap showing protein expression measured via CITE-seq using a reduced panel for convalescent donors sampled on day 35. (**B**) Violin plots showing the expression of activation markers separated by donor group and time point.

Figure S6. Transcriptomic comparison of spike-specific T cells before and after vaccination. (**A**) Proportions of $CD4^+$ T cells belonging to each $CD4^+$ T cell cluster separated by donor and time point. (**B**) GSEA summary of differentially expressed genes between $CD4^+$ T cells sampled at 6–9M versus 18M. (**C**) Percentages of $CD4^+$ T cells with expression of *IL10*. (**D**) Proportions of $CD8^+$ T cells belonging to each $CD8^+$ T cell cluster separated by donor and time point.

Figure S7. Clonal characterization of spike-specific T cells before and after vaccination. (**A**) Proportions of $CD4^+$ and $CD8^+$ T cells classified by the degree of clonal expansion. (**B**) *IFNG* expression among expanded $CD8^+$ T cell clonotypes after vaccination separated by donor.

Figure S8. Transcriptomic signatures of $CD8^+$ T cell clonotypes detected at one or both time points. (**A**) Volcano plot showing differentially expressed genes between existing and newly detected $CD8^+$ T cell clonotypes at 18M. (**B**) GSEA summary of differentially expressed genes between existing and newly detected $CD8^+$ T cell clonotypes at 18M. (**C**) GSEA plot showing significantly enriched pathways at 18M.

Figure S9. Characterization of hybrid spike-specific T cell responses in donors with CLL. (**A**) Overview of donors and sampling time points from a cohort of patients undergoing treatment for CLL. (**B**) Frequencies of AIM^+ memory $CD4^+$ T cells. (**C**) Frequencies of AIM^+ memory $CD8^+$ T cells. (**D**) Percentages of AIM^+ memory $CD4^+$ T cells expressing cytokines. (**E**) Percentages of total memory $CD8^+$ T cells expressing IFN-γ.

Figure S10. Summary of hybrid T cell immunity shaped by infection and vaccination. Schematic representation of the key findings.

Figure 1

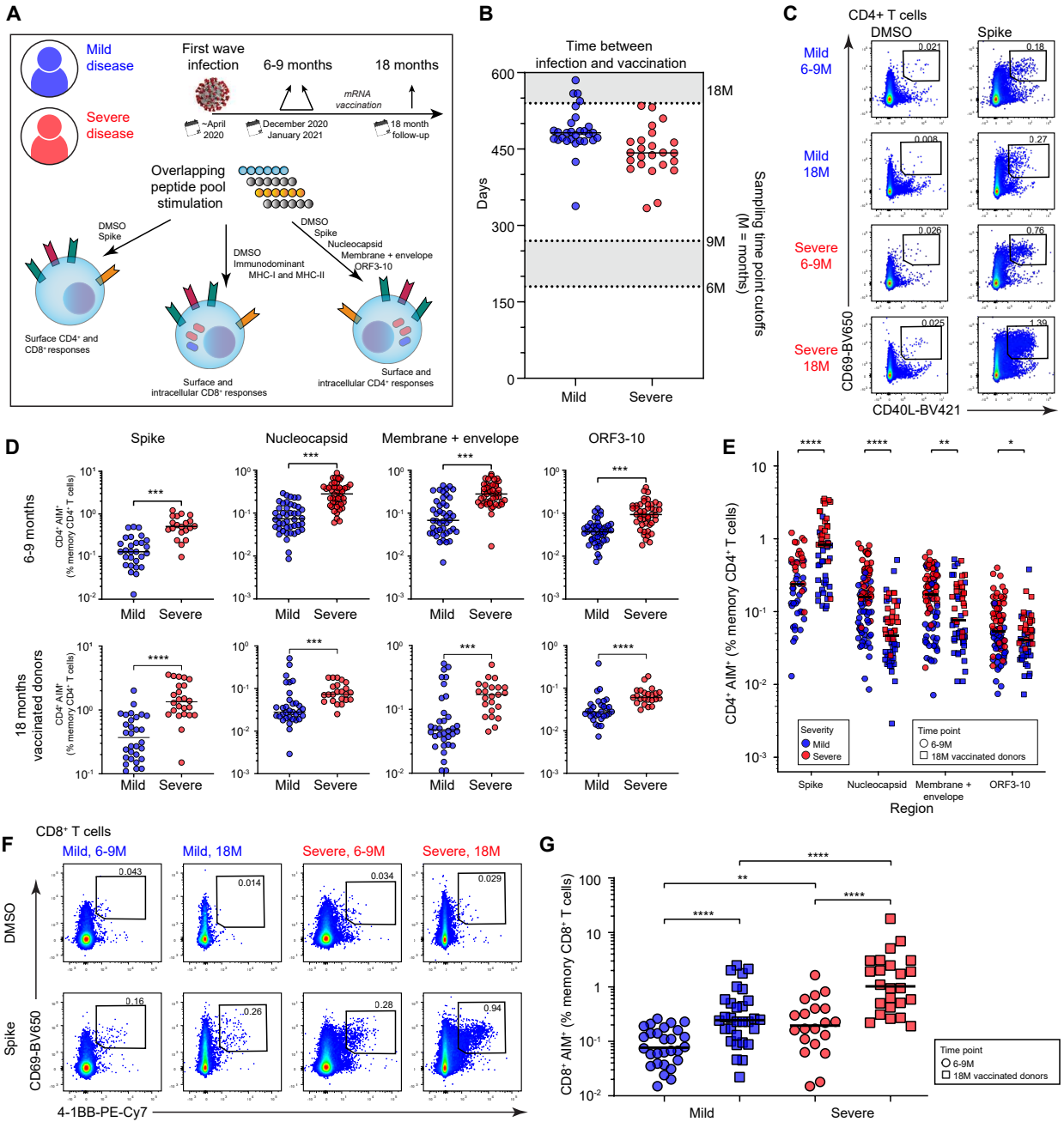
A
Mild disease
Severe disease
First wave infection
6-9 months
18 months
mRNA vaccination
~April 2020
December 2020 January 2021
18 month follow-up
Overlapping peptide pool stimulation
DMSO
Spike
DMSO
Immunodominant MHC-I and MHC-II
DMSO
Spike
Nucleocapsid
Membrane + envelope
ORF3-10
Surface CD4+ and CD8+ responses
Surface and intracellular CD8+ responses
Surface and intracellular CD4+ responses
B
Time between infection and vaccination
Days
Sampling time point cutoffs (M = months)
18M
9M
6M
Mild
Severe
C
CD4+ T cells
DMSO
Spike
Mild 6-9M
Mild 18M
Severe 6-9M
Severe 18M
CD69-BV650
CD40L-BV421
D
Spike
Nucleocapsid
Membrane + envelope
ORF3-10
6-9 months
18 months vaccinated donors
CD4+ AIM+ (% memory CD4+ T cells)
Mild
Severe
E
CD4+ AIM+ (% memory CD4+ T cells)
Severity
Mild
Severe
Time point
6-9M
18M vaccinated donors
Spike
Nucleocapsid
Membrane + envelope
ORF3-10
Region
F
CD8+ T cells
Mild, 6-9M
Mild, 18M
Severe, 6-9M
Severe, 18M
DMSO
Spike
CD69-BV650
4-1BB-PE-Cy7
G
CD8+ AIM+ (% memory CD8+ T cells)
Time point
6-9M
18M vaccinated donors
Mild
Severe

Figure 2

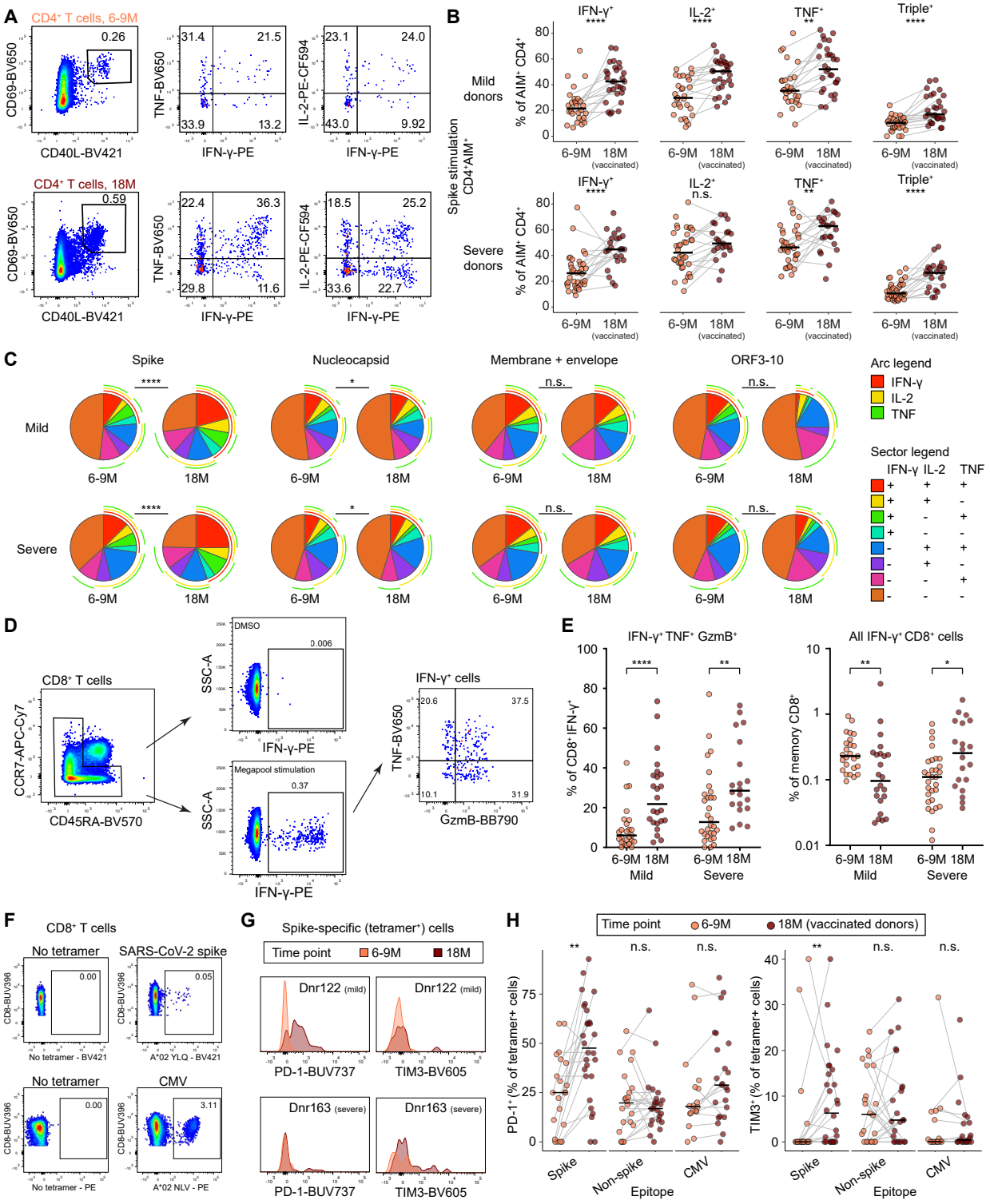
A
CD4⁺ T cells, 6-9M
CD4⁺ T cells, 18M
CD69-BV650
CD40L-BV421
TNF-BV650
IFN-γ-PE
IL-2-PE-CF594
B
Mild donors
Severe donors
Spike stimulation CD4⁺AIM⁺
% of AIM⁺ CD4⁺
IFN-γ⁺
IL-2⁺
TNF⁺
Triple⁺
6-9M 18M (vaccinated)
n.s.
C
Spike
Nucleocapsid
Membrane + envelope
ORF3-10
Mild
Severe
6-9M
18M
Arc legend
IFN-γ
IL-2
TNF
Sector legend
IFN-γ IL-2 TNF
D
CD8⁺ T cells
CCR7-APC-Cy7
CD45RA-BV570
DMSO
Megapool stimulation
SSC-A
IFN-γ-PE
IFN-γ⁺ cells
GzmB-BB790
E
IFN-γ⁺ TNF⁺ GzmB⁺
% of CD8⁺ IFN-γ⁺
All IFN-γ⁺ CD8⁺ cells
% of memory CD8⁺
Mild
Severe
F
CD8⁺ T cells
No tetramer
SARS-CoV-2 spike
CMV
CD8-BUV396
No tetramer - BV421
A*02 YLQ - BV421
No tetramer - PE
A*02 NLV - PE
G
Spike-specific (tetramer⁺) cells
Time point 6-9M 18M
Dnr122 (mild)
Dnr163 (severe)
PD-1-BUV737
TIM3-BV605
H
Time point 6-9M 18M (vaccinated donors)
PD-1⁺ (% of tetramer+ cells)
TIM3⁺ (% of tetramer+ cells)
Spike
Non-spike
CMV
Epitope

Figure 3

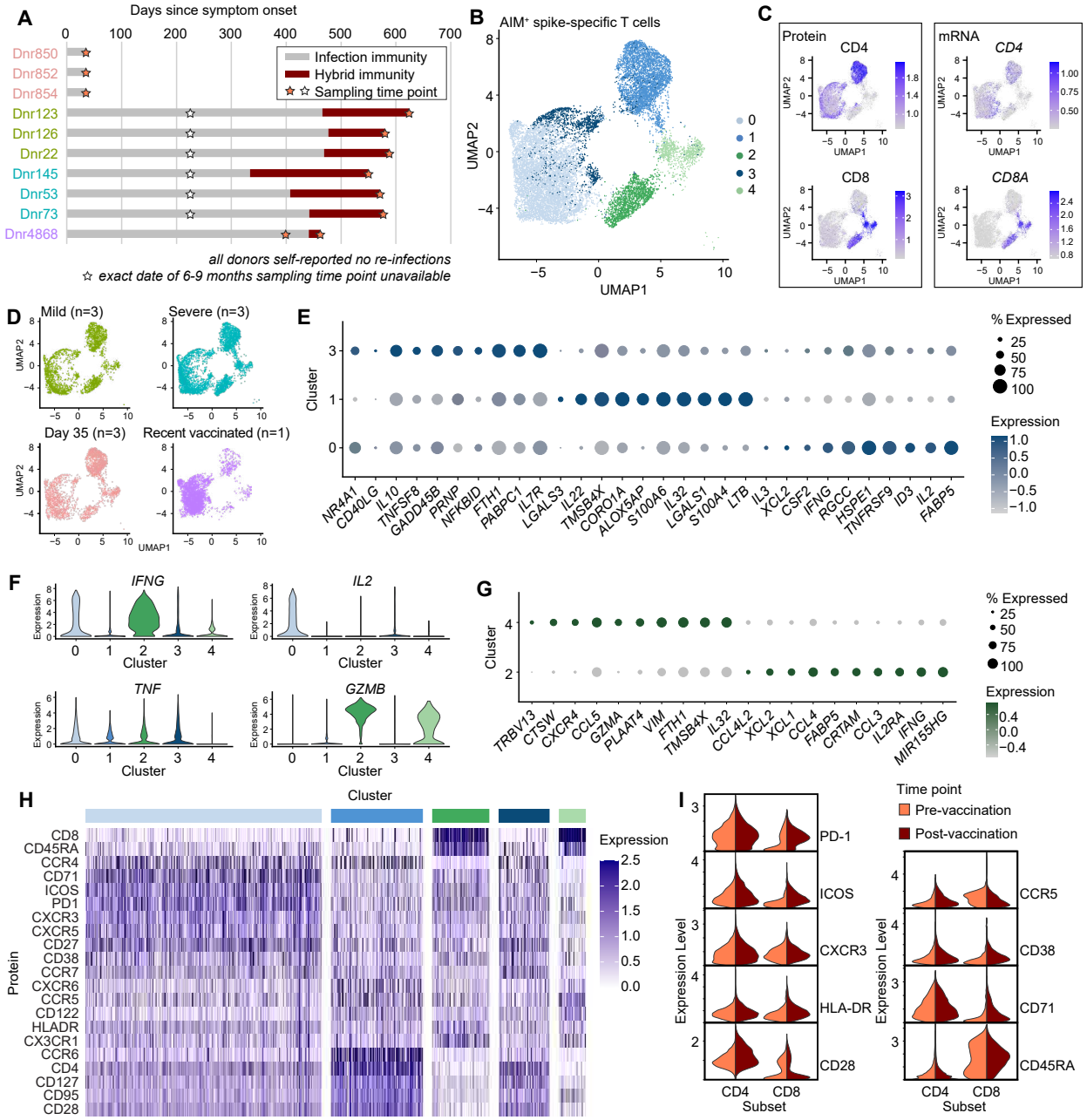
A
Days since symptom onset
Infection immunity
Hybrid immunity
Sampling time point
Dnr850
Dnr852
Dnr854
Dnr123
Dnr126
Dnr22
Dnr145
Dnr53
Dnr73
Dnr4868
all donors self-reported no re-infections
exact date of 6-9 months sampling time point unavailable
B
AIM+ spike-specific T cells
UMAP1
UMAP2
C
Protein
mRNA
CD4
CD8
CD8A
D
Mild (n=3)
Severe (n=3)
Day 35 (n=3)
Recent vaccinated (n=1)
E
Cluster
% Expressed
Expression
F
IFNG
IL2
TNF
GZMB
G
H
Protein
Expression
I
Time point
Pre-vaccination
Post-vaccination
PD-1
ICOS
CXCR3
HLA-DR
CD28
CCR5
CD38
CD71
CD45RA
Expression Level
Subset

Figure 4

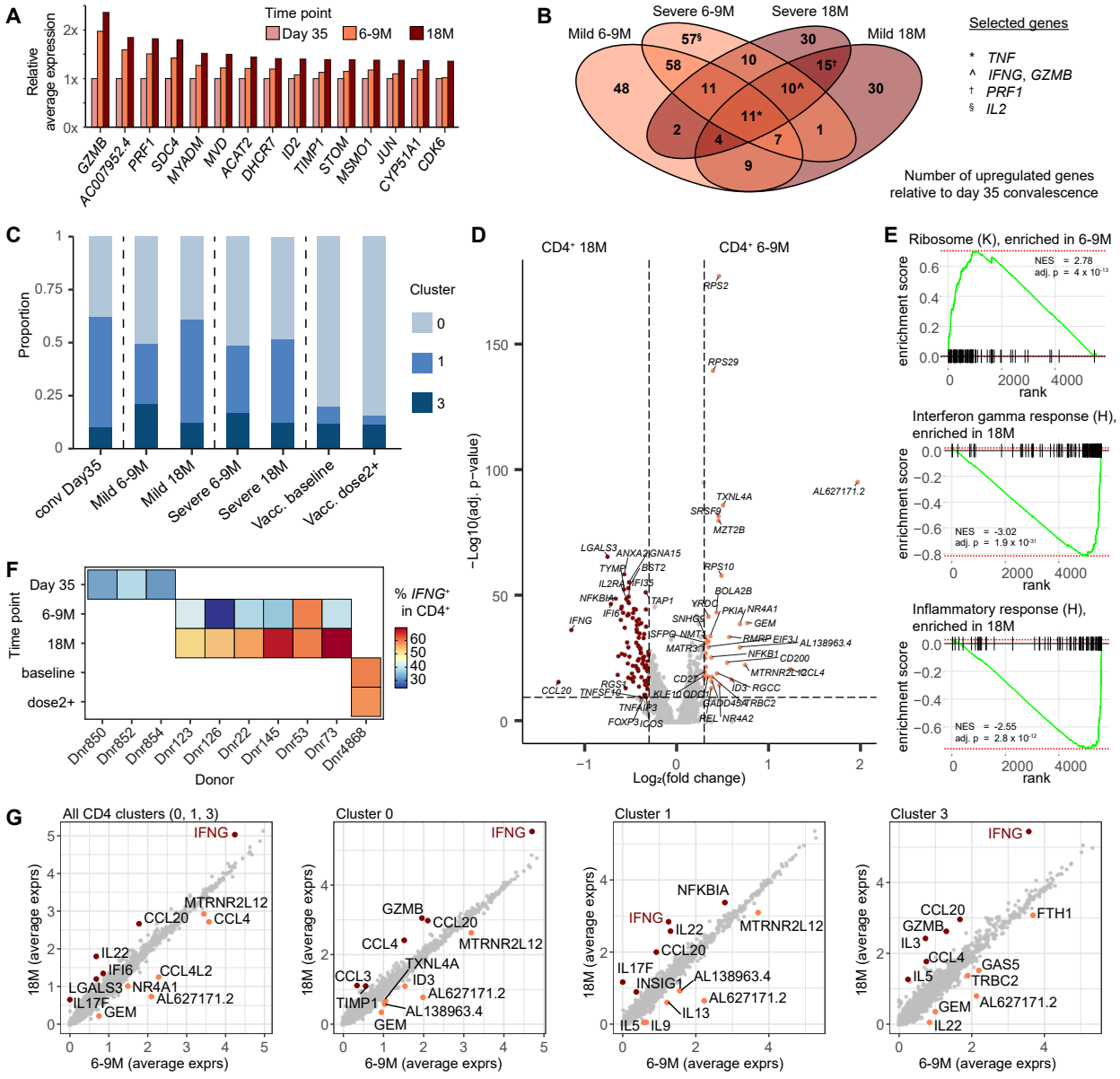
A
Time point
Day 35
6-9M
18M
Relative average expression
2x
1x
0x
GZMB
AC007952.4
PRF1
SDC4
MYADM
MVD
ACAT2
DHCR7
ID2
TIMP1
STOM
MSMO1
JUN
CYP51A1
CDK6
B
Mild 6-9M
Severe 6-9M
Severe 18M
Mild 18M
48
57§
58
10
30
15†
11
10^
30
2
11*
4
7
1
9
Selected genes
* TNF
^ IFNG, GZMB
† PRF1
§ IL2
Number of upregulated genes relative to day 35 convalescence
C
Proportion
Cluster
0
1
3
conv Day35
Mild 6-9M
Mild 18M
Severe 6-9M
Severe 18M
Vacc. baseline
Vacc. dose2+
D
CD4⁺ 18M
CD4⁺ 6-9M
−Log10(adj. p−value)
Log₂(fold change)
RPS2
RPS29
AL627171.2
TXNL4A
SRSF9
MZT2B
RPS10
BOLA2B
YRDC
PKIA
NR4A1
GEM
AL138963.4
CD200
MTRNR2L12
CCL4
ID3
RGCC
GADD45A
TRBC2
NR4A2
ICOS
FOXP3
TNFAIP3
KLF10
CD27
TNFSF9
CCL20
RGS1
IFNG
IFI6
TAP1
NFKBIA
IFI35
BST2
TYMP
LGALS3
ANXA2
IGNA15
E
Ribosome (K), enriched in 6-9M
NES = 2.78
adj. p = 4 x 10⁻¹³
Interferon gamma response (H), enriched in 18M
NES = -3.02
adj. p = 1.9 x 10⁻³¹
Inflammatory response (H), enriched in 18M
NES = -2.55
adj. p = 2.8 x 10⁻¹²
enrichment score
rank
F
Time point
Day 35
6-9M
18M
baseline
dose2+
% IFNG⁺ in CD4⁺
Donor
Dnr850
Dnr852
Dnr854
Dnr123
Dnr126
Dnr22
Dnr145
Dnr53
Dnr73
Dnr4868
G
All CD4 clusters (0, 1, 3)
Cluster 0
Cluster 1
Cluster 3
18M (average exprs)
6-9M (average exprs)
IFNG
MTRNR2L12
CCL20
CCL4
IL22
IFI6
CCL4L2
LGALS3
NR4A1
AL627171.2
IL17F
GEM
GZMB
TXNL4A
ID3
CCL3
TIMP1
NFKBIA
IL22
INSIG1
IL17F
IL13
IL5
IL9
FTH1
IL3
GAS5
TRBC2
IL5

Figure 5

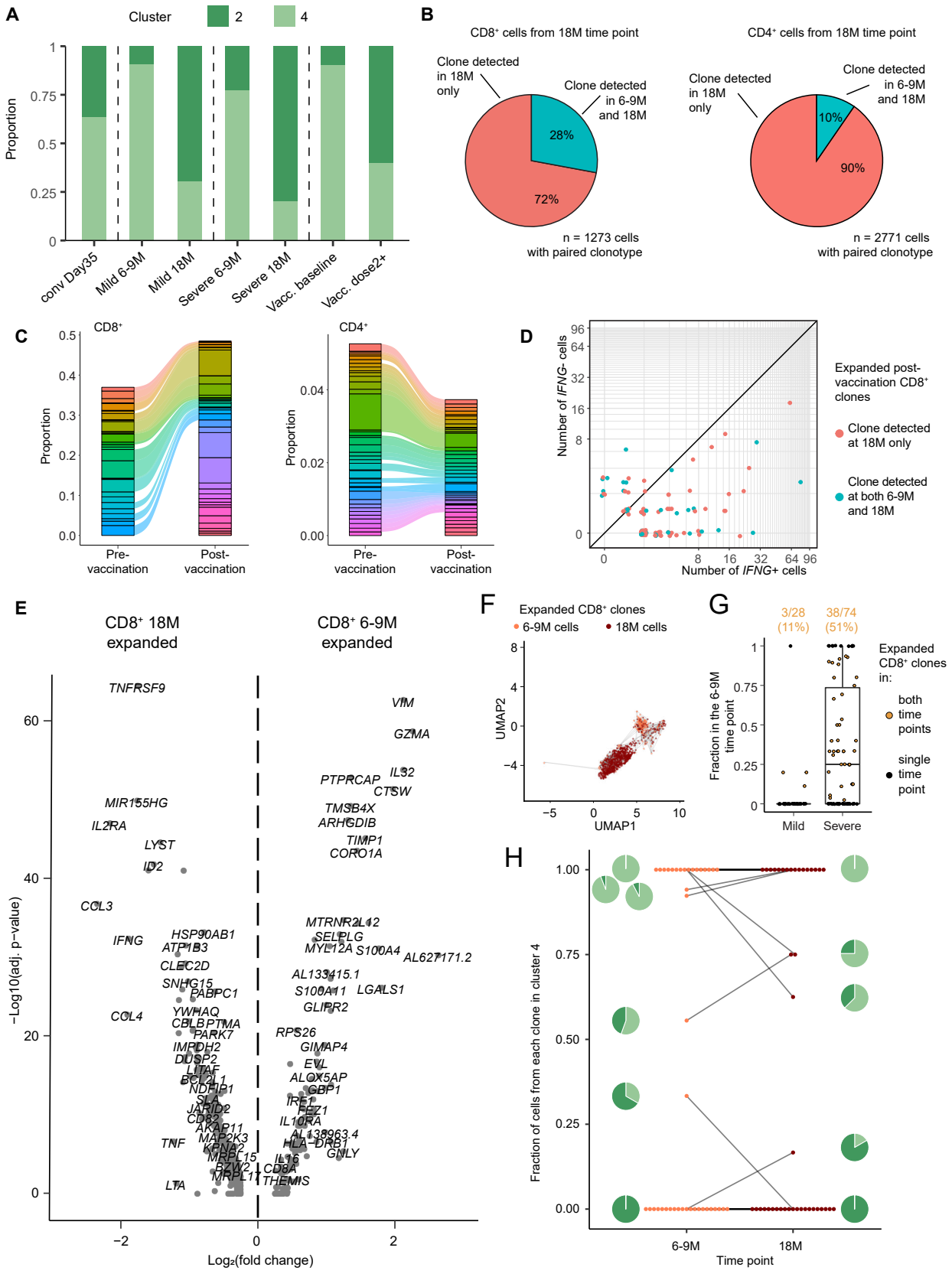
A
Cluster
2
4
Proportion
conv Day35
Mild 6-9M
Mild 18M
Severe 6-9M
Severe 18M
Vacc. baseline
Vacc. dose2+
B
CD8⁺ cells from 18M time point
Clone detected in 18M only
Clone detected in 6-9M and 18M
28%
72%
n = 1273 cells with paired clonotype
CD4⁺ cells from 18M time point
Clone detected in 18M only
Clone detected in 6-9M and 18M
10%
90%
n = 2771 cells with paired clonotype
C
CD8⁺
CD4⁺
Proportion
Pre-vaccination
Post-vaccination
D
Number of IFNG- cells
Number of IFNG+ cells
Expanded post-vaccination CD8⁺ clones
Clone detected at 18M only
Clone detected at both 6-9M and 18M
E
CD8⁺ 18M expanded
CD8⁺ 6-9M expanded
−Log10(adj. p−value)
Log₂(fold change)
TNFRSF9
MIR155HG
IL2RA
LYST
ID2
CCL3
IFNG
CCL4
TNF
LTA
VIM
GZMA
IL32
PTPRCAP
CTSW
TMSB4X
ARHGDIB
TIMP1
CORO1A
S100A4
AL627171.2
S100A11
LGALS1
GLIPR2
RPS26
GIMAP4
EVL
ALOX5AP
GBP1
IRF1
PEF1
IL10RA
HLA-DRB1
GNLY
CD8A
F
Expanded CD8⁺ clones
6-9M cells
18M cells
UMAP1
UMAP2
G
3/28 (11%)
38/74 (51%)
Fraction in the 6-9M time point
Mild
Severe
Expanded CD8⁺ clones in:
both time points
single time point
H
Fraction of cells from each clone in cluster 4
6-9M
18M
Time point

Figure 6

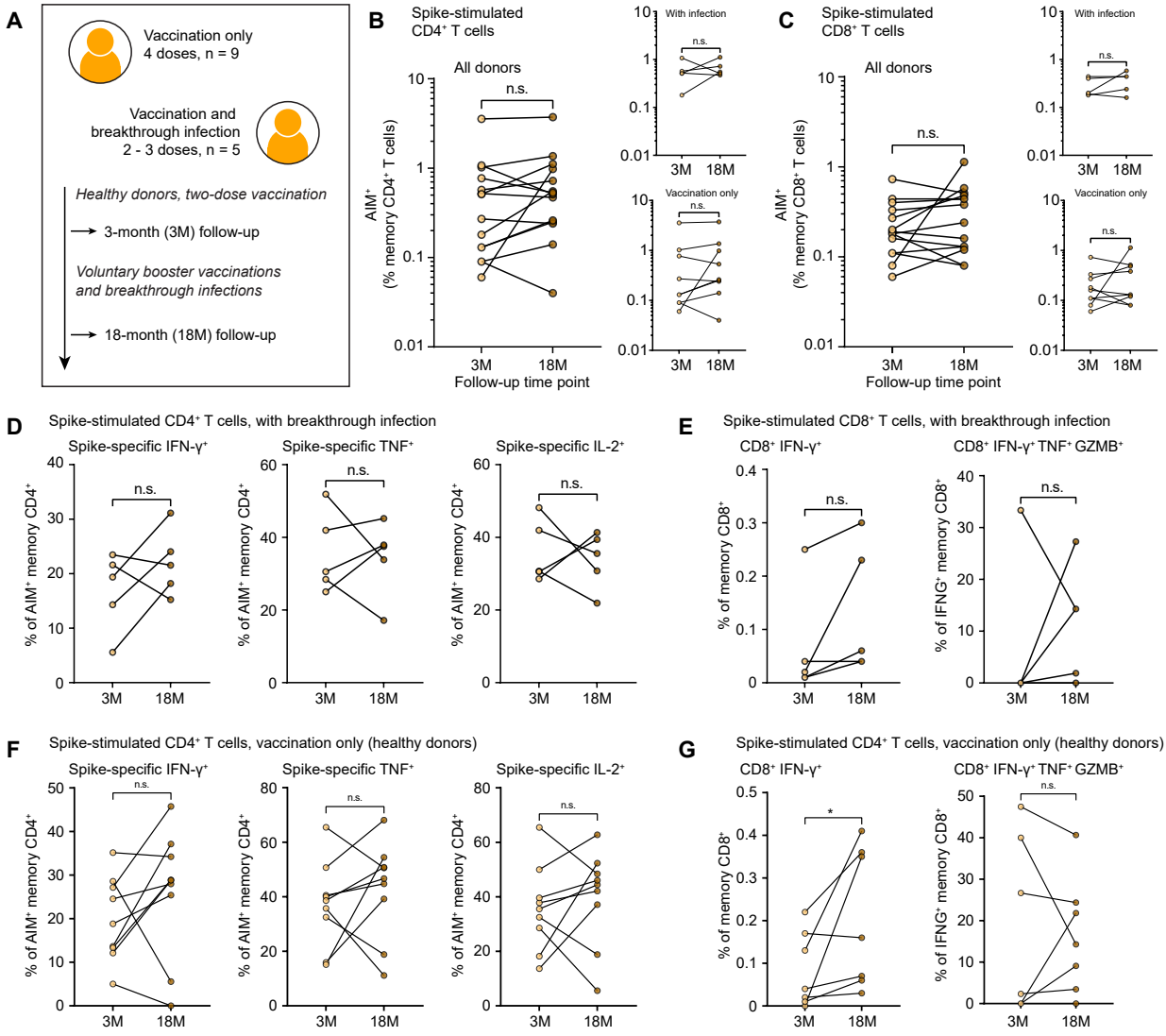
A
Vaccination only
4 doses, n = 9
Vaccination and
breakthrough infection
2 - 3 doses, n = 5
Healthy donors, two-dose vaccination
3-month (3M) follow-up
Voluntary booster vaccinations
and breakthrough infections
18-month (18M) follow-up
B
Spike-stimulated
CD4+ T cells
All donors
With infection
Vaccination only
AIM+
(% memory CD4+ T cells)
n.s.
3M
18M
Follow-up time point
C
Spike-stimulated
CD8+ T cells
All donors
With infection
Vaccination only
AIM+
(% memory CD8+ T cells)
n.s.
3M
18M
Follow-up time point
D
Spike-stimulated CD4+ T cells, with breakthrough infection
Spike-specific IFN-γ+
Spike-specific TNF+
Spike-specific IL-2+
% of AIM+ memory CD4+
n.s.
3M
18M
E
Spike-stimulated CD8+ T cells, with breakthrough infection
CD8+ IFN-γ+
CD8+ IFN-γ+ TNF+ GZMB+
% of memory CD8+
% of IFNG+ memory CD8+
n.s.
3M
18M
F
Spike-stimulated CD4+ T cells, vaccination only (healthy donors)
Spike-specific IFN-γ+
Spike-specific TNF+
Spike-specific IL-2+
% of AIM+ memory CD4+
n.s.
3M
18M
G
Spike-stimulated CD4+ T cells, vaccination only (healthy donors)
CD8+ IFN-γ+
CD8+ IFN-γ+ TNF+ GZMB+
% of memory CD8+
% of IFNG+ memory CD8+
*
n.s.
3M
18M

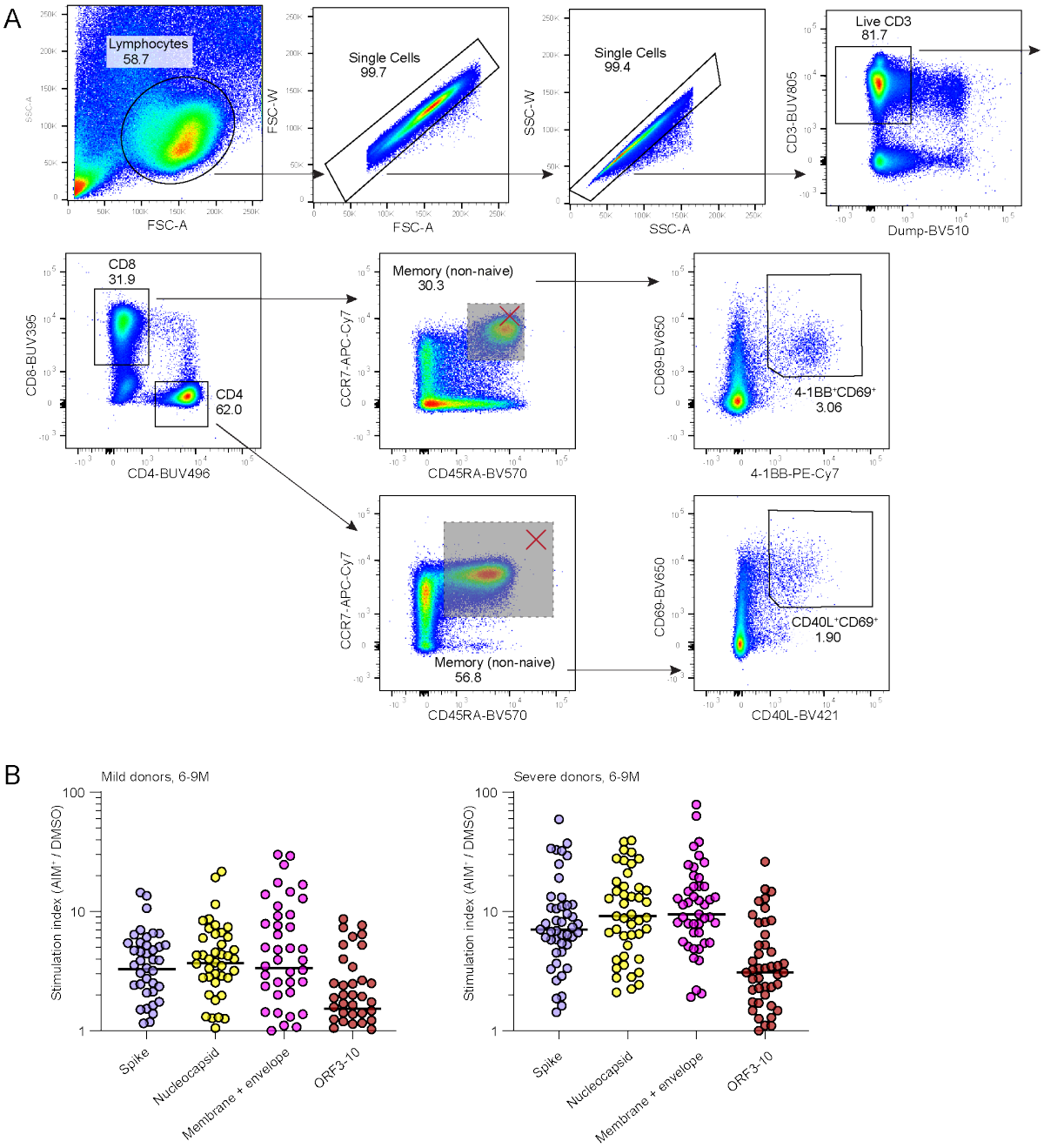

Fig. S1. Detection of AIM⁺ T cells. (**A**) Representative gating strategy for the identification of AIM⁺ CD4⁺ and CD8⁺ T cells from flow cytometry of peripheral blood mononuclear cells. (**B**) Stimulation index of individual donor responses from 6-9M.

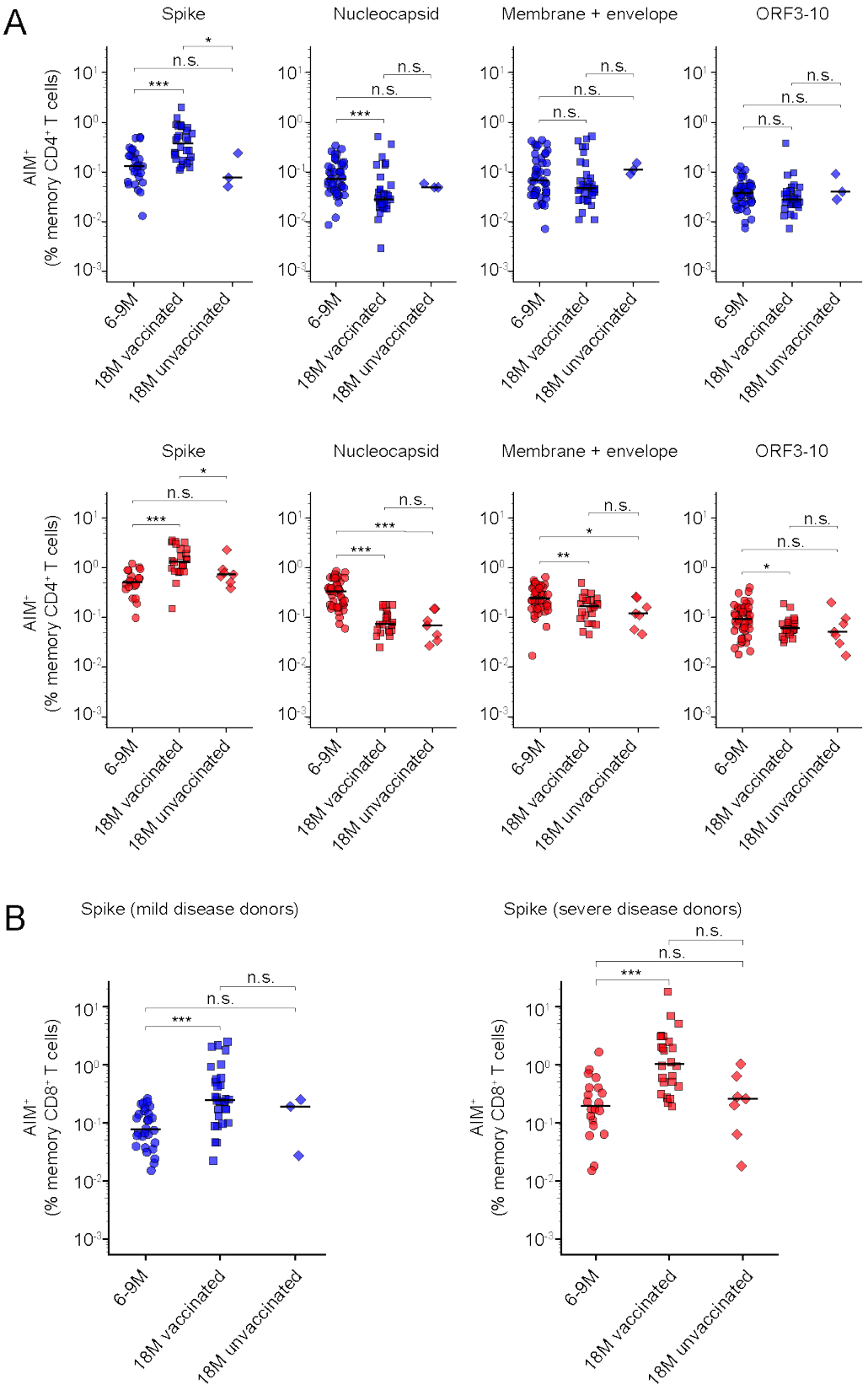

Fig. S2. Effect of vaccination on the frequency of spike-specific T cells. (**A**) Frequency of AIM$^+$ CD4$^+$ T cell populations targeting different regions of SARS-CoV-2. (**B**) Frequency of AIM+ CD8+ T cell populations after (SARS-CoV-2 spike) peptide pool stimulation.

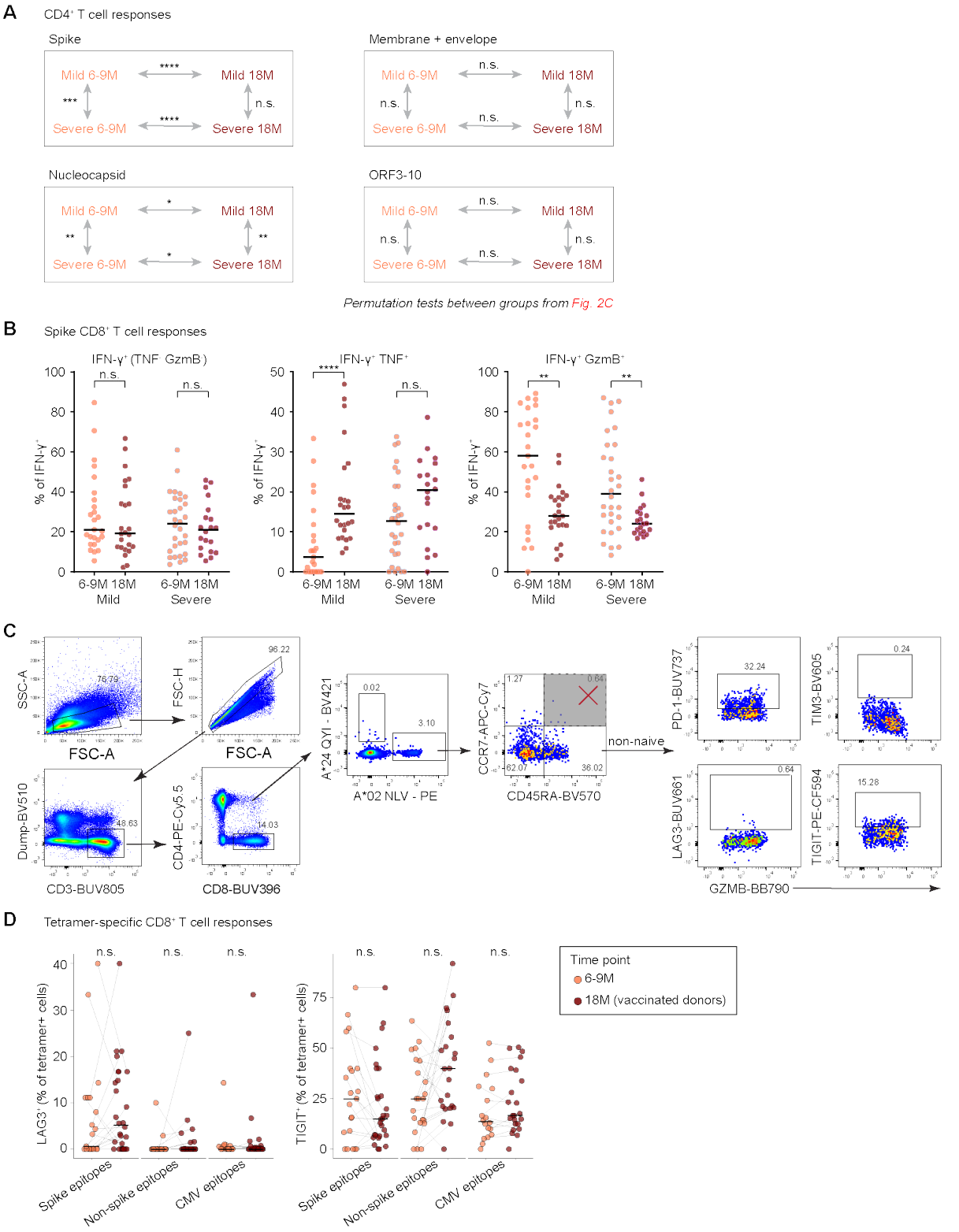

Fig. S3. Characterization of T cell cytokine production and co-inhibitory receptor expression. (**A**) Permutation test comparisons of AIM⁺ CD4⁺ T cell cytokine co-expression profiles (related to Fig. 2C). (**B**) Percentage of IFN-γ⁺ memory CD8⁺ T cells with polyfunctional cytokine expression after spike peptide pool stimulation. (**C**) Representative flow plots of inhibitory marker gating from tetramer-specific CD8⁺ T cell populations. (**D**) Percentage of tetramer-specific CD8⁺ T cells with inhibitory marker expression.

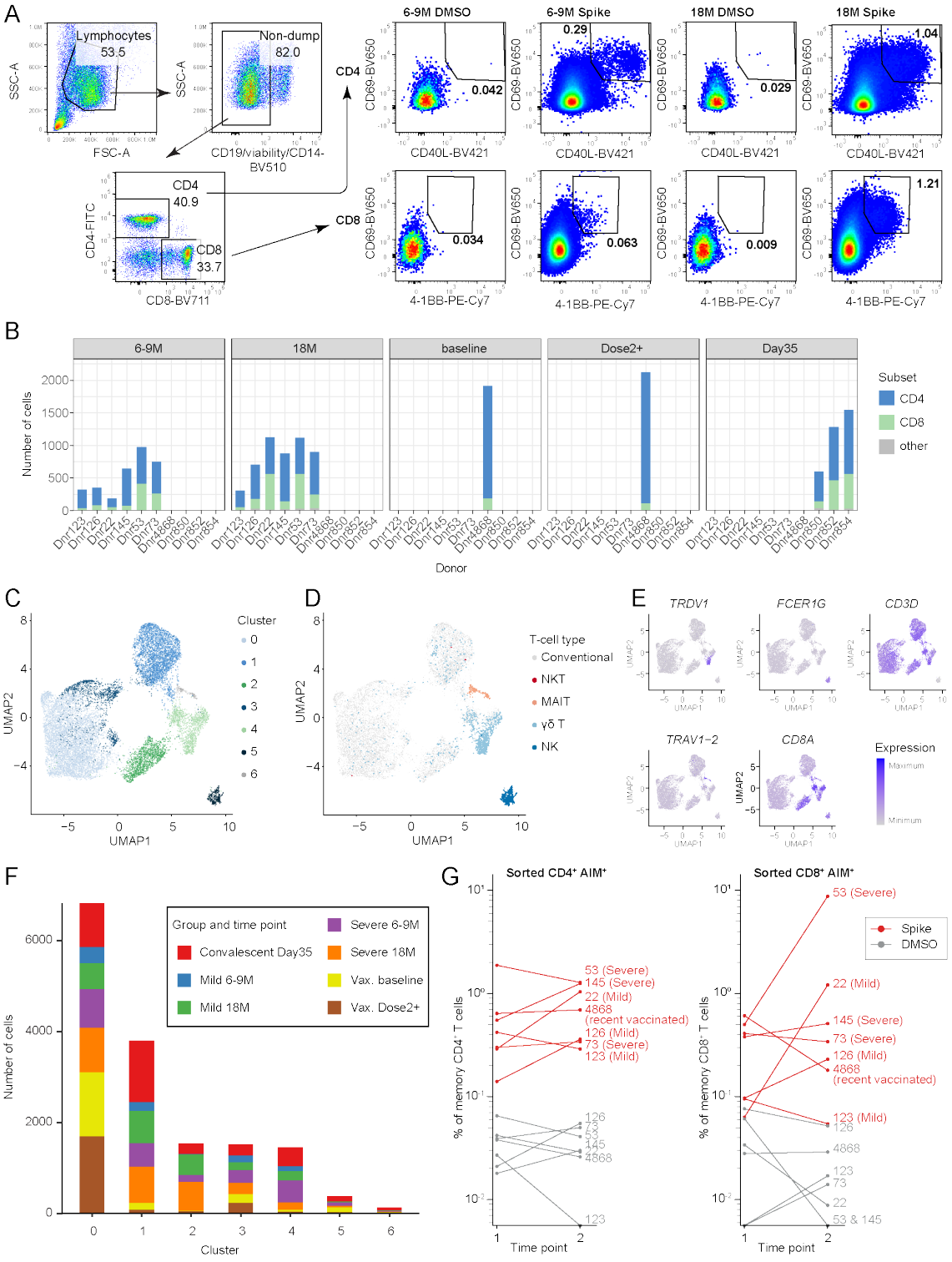

Fig. S4. Classification of AIM⁺ populations sorted for scRNA-seq. (**A**) Representative gating strategy for the identification and sorting of AIM⁺ CD4⁺ and CD8⁺ T cells for input to scRNA-seq. (**B**) Distribution of cells with CD4 or CD8 protein expression between individual donors and time points. Other includes cells with double positive or double negative CD4/CD8 expression. (**C**) UMAP and clustering of all sorted cells including unconventional T cell subsets. (**D**) Classification of unconventional T cell subsets. (**E**) Expression of transcripts corresponding to conventional and unconventional T cell subsets. (**F**) Distribution of donor groups and time points between each UMAP cluster. (**G**) Frequency of sorted AIM+ populations as determined by flow cytometry. Time points 1 and 2 correspond to pre- and post-vaccination respectively.

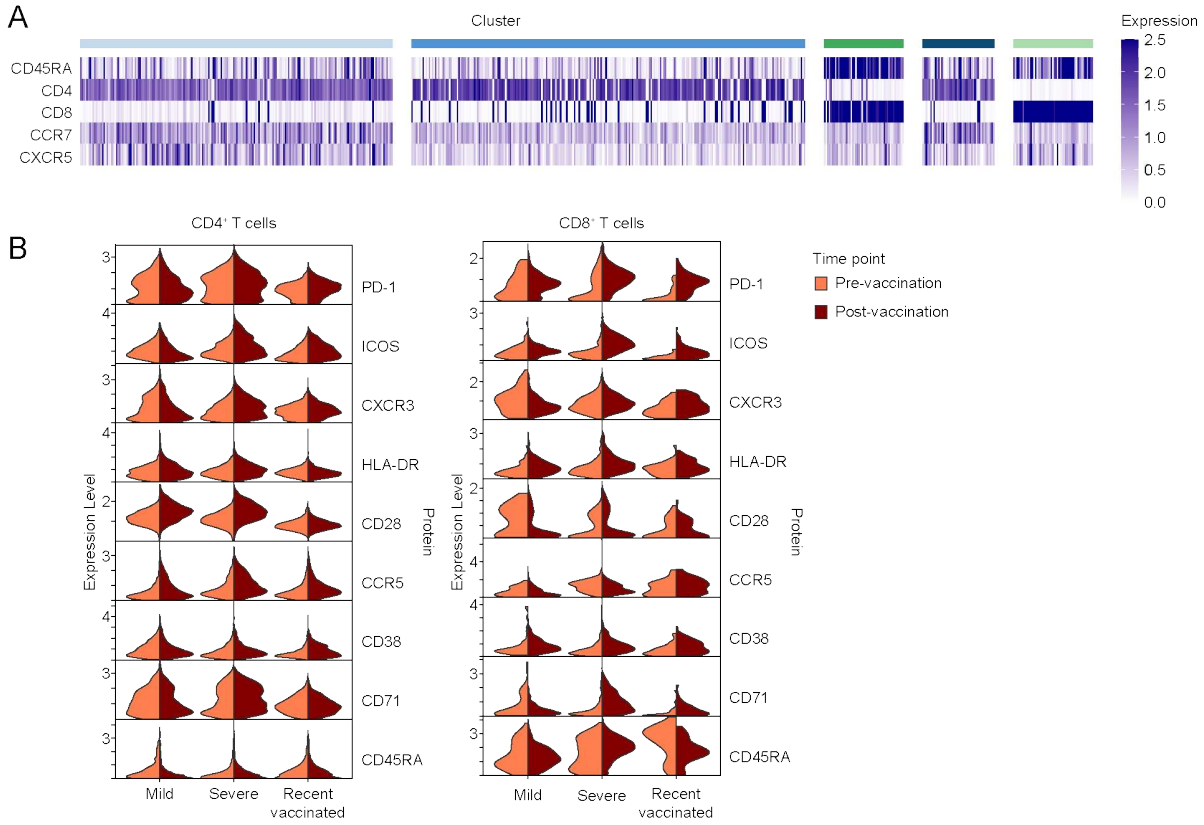

Fig. S5. Protein expression of spike-specific T cells from CITE-seq analyses. (**A**) Heatmap of protein expression measured by nucleotide-conjugated antibodies for convalescent donors at Day 35 using a reduced panel of markers. (**B**) Violin plots of expression for activation markers separated by donor groups and split by time point.

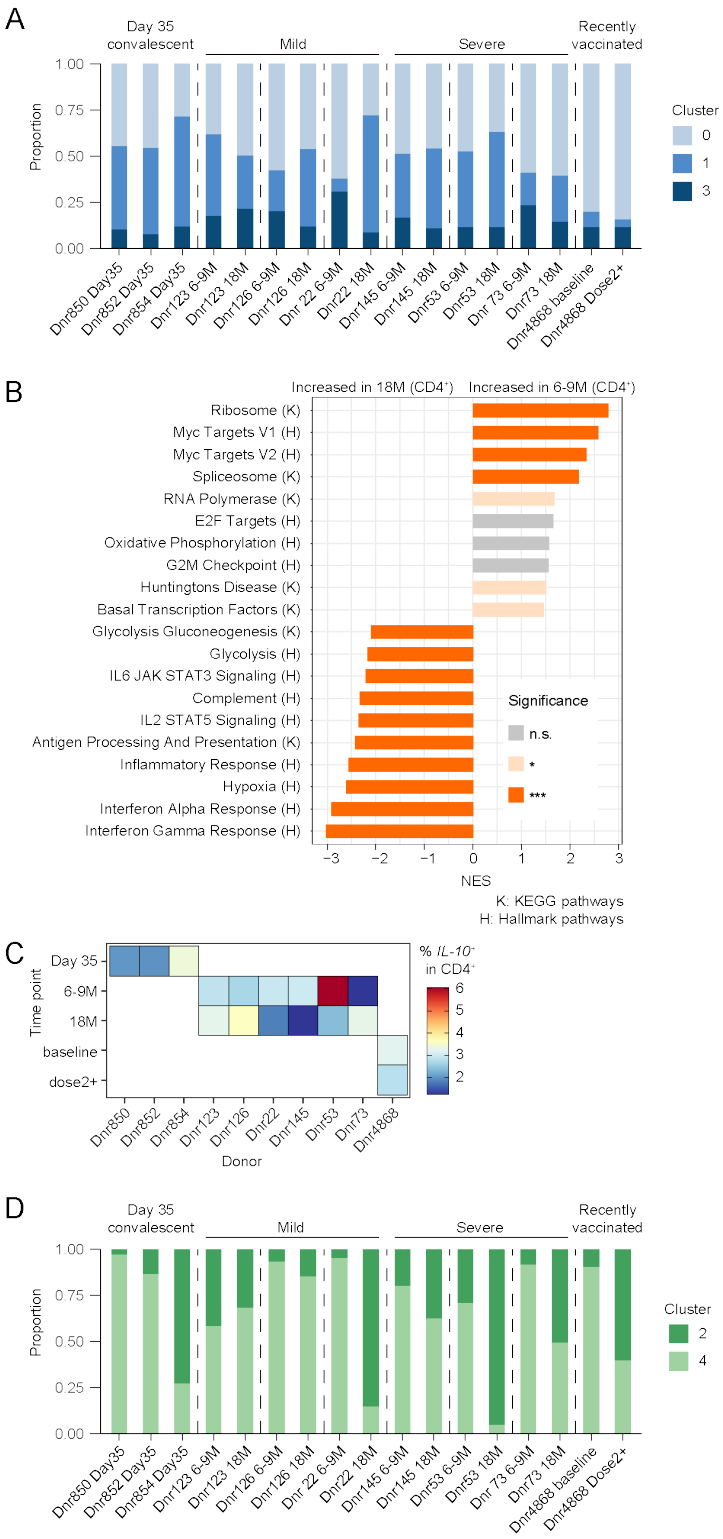

Fig. S6. Comparison of pre- and post-vaccination T cell responses. (**A**) Proportion of sequenced CD4⁺ T cells belonging to each CD4⁺ T cell cluster, shown at the individual donor and time point level. (**B**) GSEA summary of differentially expressed genes between CD4⁺ T cells from 6-9M and 18M. (**C**) Percentage of CD4⁺ T cells with expression for *IL-10*. (**D**) Proportion of sequenced CD8⁺ T cells belonging to each CD8⁺ T cell cluster, shown at the individual donor and time point level.

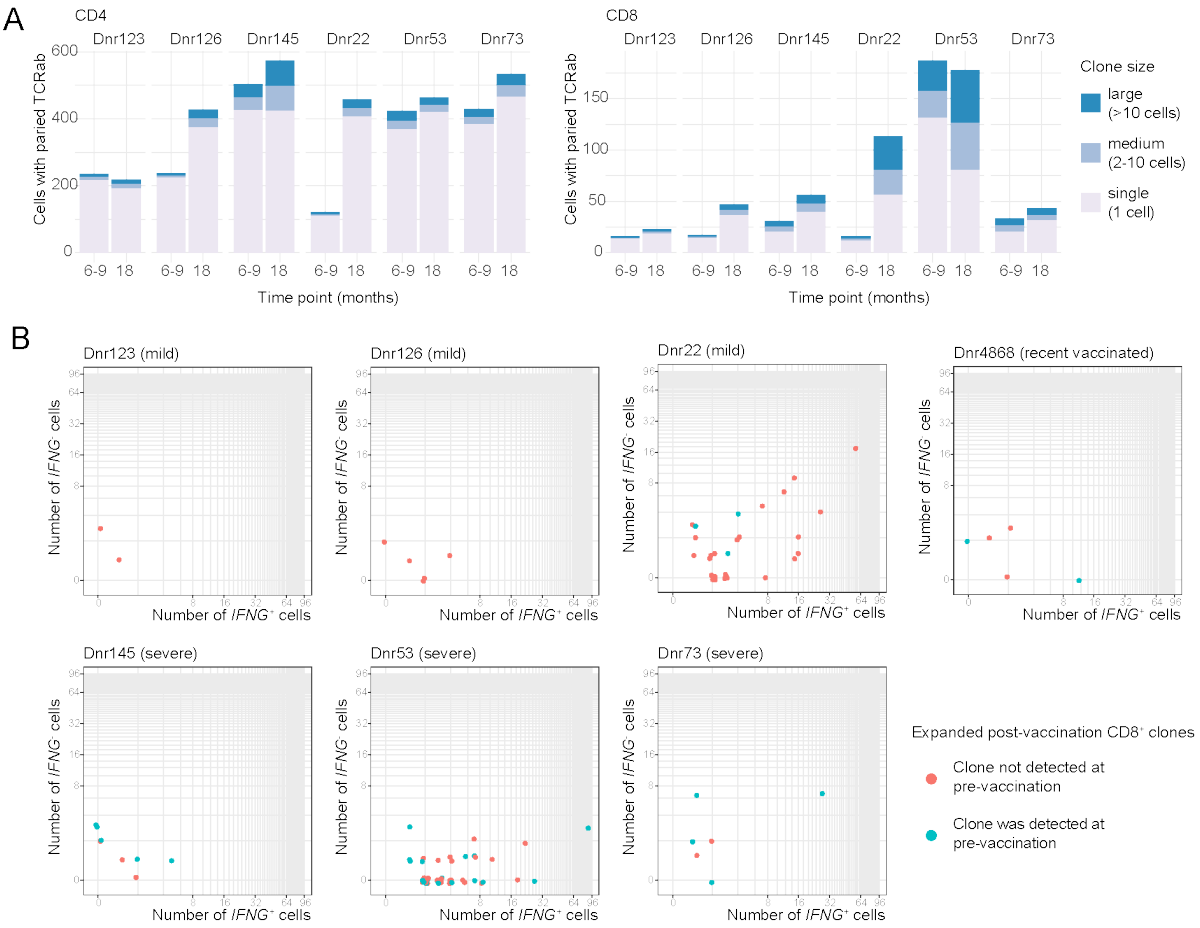

Fig. S7. Clonal characterization of spike-specific CD4⁺ and CD8⁺ T cells. (**A**) Proportion of cells from the CD4⁺ and CD8⁺ T cell subsets classified according to their degree of clonal expansion. (**B**) Expanded CD8⁺ T cell clones from the post-vaccination time point of each donor showing the number of constituent cells with positive *IFNG* expression. Clones were colored based on whether they were detected in the pre-vaccination time point.

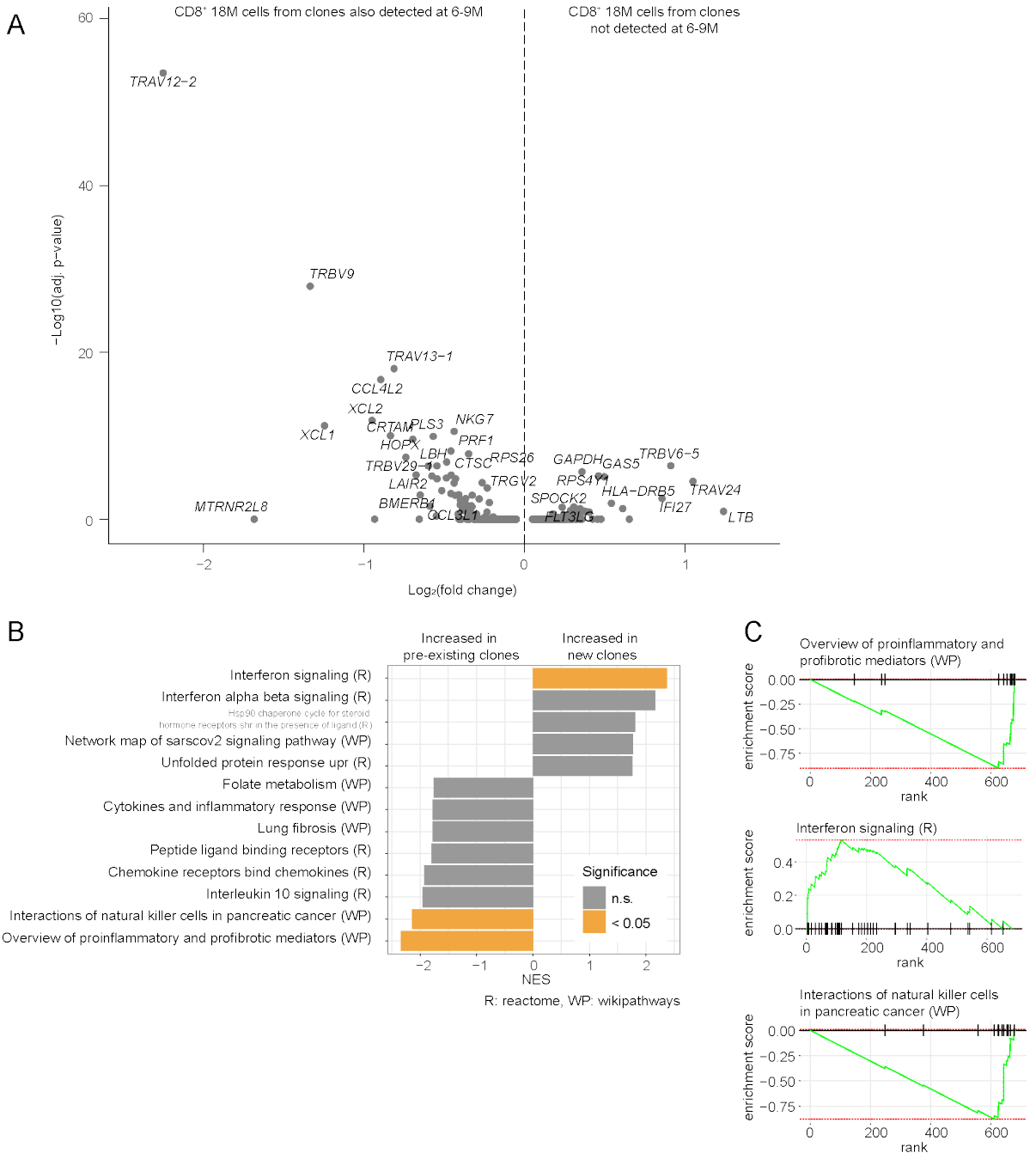

Fig. S8. Transcriptomic signatures of CD8⁺ T cell clones detected in one or both time points. (**A**) Volcano plot of differentially expressed genes between 18M pre-existing and newly detected clones. (**B**) GSEA summary of differentially expressed genes between18M pre-existing and newly detected clones. (**C**) GSEA enrichment plot of statistically significant pathways.

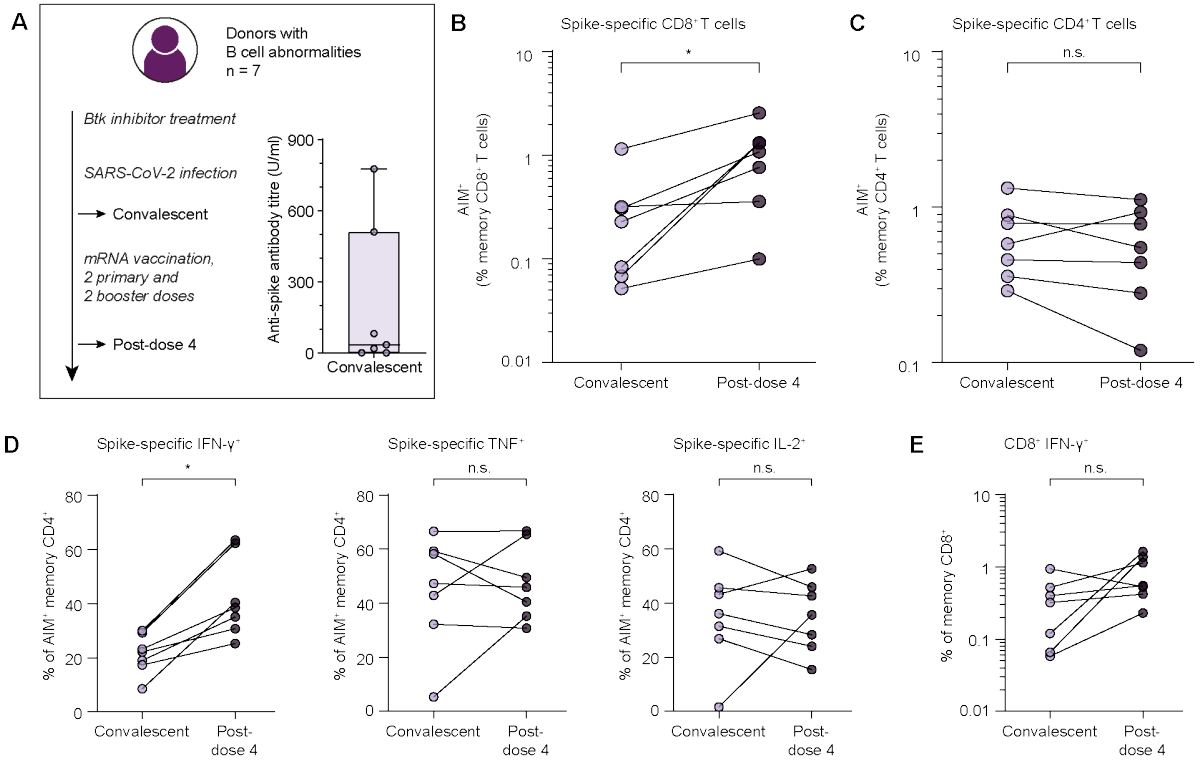

Fig. S9. Limited boosting of T cell responses after initial infection and four-dose vaccination in a cohort of donors with CLL. (**A**) Overview of donors and sampling time points selected from a cohort of patients treated for chronic lymphocytic leukemia (**B**) Frequency of spike-specific $CD4^+$ T cells. (**C**) Frequency of spike-specific $CD8^+$ T cells. (**D**) Percentage of spike-specific $CD4^+$ T cells expressing cytokines. (**E**) Percentage of total memory $CD8^+$ T cells expressing IFN-γ.

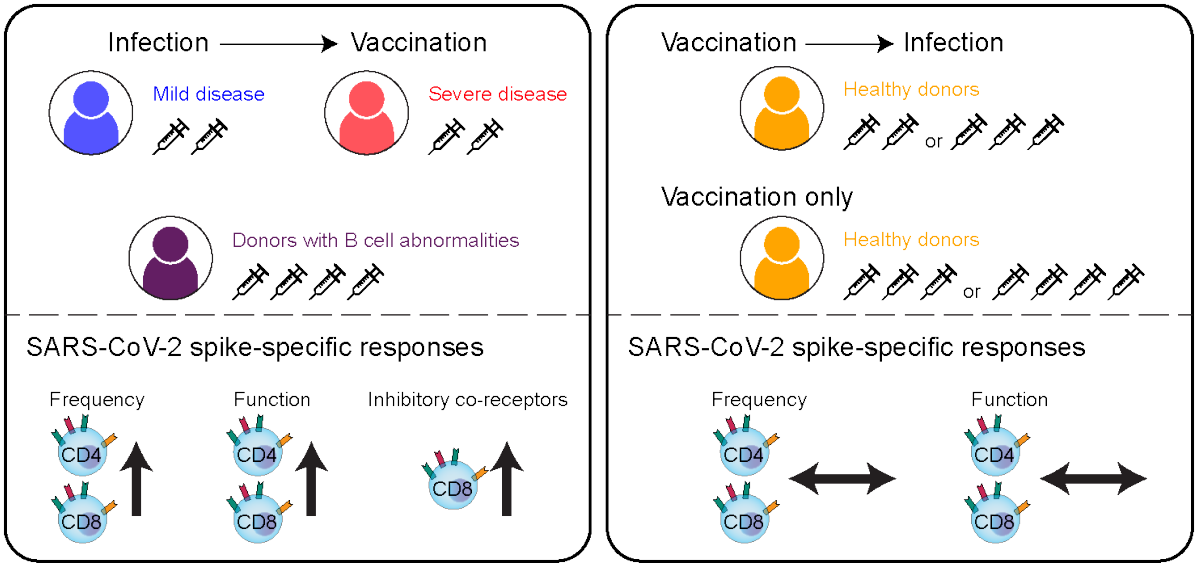

Fig. S10. Summary of the role of SARS-CoV-2 infection and vaccination in shaping T cell responses. Schematic summarizing key findings.

Table S1. Summary of donors from the mild and severe disease cohorts.

Donor group and time point	Characteristic	Value
Mild (non-hospitalized)	Total number	50
	Number with paired time points	31
6-9 months convalescence	Total number	44
	Unvaccinated	44
	Median age at infection (range)	54.5 (43−78)
	Male / Female	33 / 11 (75/25 %)
18 months convalescence	Total number	37
	Unvaccinated	3
	Vaccinated	34
	Vaccine platform (Comirnaty, SpikeVax, Vaxzevria, unknown)	27, 3, 2, 2
	Median age at infection (range)	57 (43−78)
	Male / Female	28 / 9 (76/24 %)
Severe (hospitalized)	Total number	53
	Number with paired time points	24
6-9 months convalescence *	Total number	45
	Unvaccinated	45
	Median age at infection (range)	57 (33−68)
	Male / Female *	34 / 7 (76/16 %)
	Admitted to ICU	26
	Required ventilator	21
18 months convalescence	Total number	32
	Unvaccinated	7
	Vaccinated	25
	Vaccine platform (Comirnaty, SpikeVax, Vaxzevria, unknown)	16, 6, 0, 3
	Median age at infection (range)	57.5 (33−76)
	Male / Female	23 / 9 (72/28 %)
	Admitted to ICU	18
	Required ventilator	15

The exact date of infection or vaccination was unavailable for 4 mild donors and 2 severe donors. *Clinical information was unavailable from 4 donors. ICU: intensive care unit.

Table S2. Summary of donors selected for tetramer analysis

Donor group and time point	Characteristic	Value
Mild (non-hospitalized) • Paired 6-9M and 18M time points for each donor • All donors vaccinated at the 18M time point	Total number	14
	Median age at infection (range)	54 (43−66)
	Male / Female	10 / 4
	HLA combinations	
	A24	3
	A2 A24	6
	A2 B7	2
	A24 B7	2
	A2 A24 B7	1
Severe (hospitalized) • Paired 6-9M and 18M time points for each donor • All donors vaccinated at the 18M time point	Total number	14
	Median age at infection (range)	57.5 (33−68)
	Male / Female	11 / 3
	HLA combinations	
	A2	5
	A24	5
	A2 A24	2
	A2 B7	1
	A2 A24 B7	1

Table S3. Summary of donors selected for single-cell RNA-sequencing

Donor group and time point	Characteristic	Value
Mild	Donor IDs	22, 123, 126
• Non-hospitalized	Age	67, 59, 57
• 6-9 months convalescence	Sex	M, M, M
• 18 months convalescence	Vaccine platform	
	Vaxzevria (Donor IDs)	22
	Comirnaty (Donor IDs)	123, 126
Severe	Donor IDs	53, 73, 145
• Non-hospitalized	Age	56, 62, 56
• 6-9 months convalescence	Sex	M, F, F
• 18 months convalescence	Vaccine platform	
	Comirnaty (Donor IDs)	53, 73
	Unknown (Donor IDs)	145
Recently vaccinated	Donor IDs	4868
• Non-hospitalized	Age	54
• Baseline: 2 weeks before vaccination or 13 months convalescence	Sex	F
	Vaccine platform	
• Dose 2+: 2 weeks after second dose vaccination or 15 months convalescence	SpikeVax (Donor IDs)	4868
Recently convalescent	Donor IDs	850, 852, 854
• Non-hospitalized	Unvaccinated	3
• Day 35 convalescence	Age	Unavailable
• Unvaccinated	Sex	F, F, M

Table S4. Summary of donors with B cell abnormalities.

Donor group and time point	Characteristic	Value
B cell abnormality	Total number	7
• Treated with Btk inhibition for CLL	Median age at convalescent time point (range)	69 (46−77)
• Convalescent	Male / Female	4 / 3
• Post-dose 4	Hospitalized	6

CLL: chronic lymphocytic leukemia, Btk: Bruton's tyrosine kinase

Table S5. Summary of healthy control vaccination cohort.

Donor group and time point	Characteristic	Value
Vaccinated healthy controls	Total number	14
• 3 month post-vaccination follow-up (two doses received)		
• 18 month post-vaccination follow-up (three or four doses received)		
With breakthrough infection	Total number	5
	Median age at vaccination (range)	32 (26−55)
	Male / Female	2 / 3
	Vaccine platform	
	Comirnaty only	2
	Comirnaty and SpikeVax	3
	Clinical history	
	Two doses > breakthrough	1
	Two doses > breakthrough > third dose	1
	Three doses > breakthrough	3
Without breakthrough infection	Total number	9
• All received 4 doses of vaccination by the 18 month follow-up	Median age at vaccination (range)	46 (28−59)
	Male / Female	4 / 5
	Vaccine platform	
	Comirnaty only	6
	Comirnaty and SpikeVax	3

Table S6. Protocol for surface staining for flow cytometry.

STEP 1: Stain for viability at room temperature for 10 minutes.					
Marker	**Fluorophore**	**Supplier**	**Dilution**	**Product number**	**Clone**
LIVE/DEAD fixable aqua	For 405 nm excitation	Invitrogen	1X in PBS	L34957	-
STEP 2: Stain for chemokine receptors at 37°C for 10 minutes.					
Marker	**Fluorophore**	**Supplier**	**Dilution**	**Product number**	**Clone**
CCR7	APC-Cy7	BioLegend	1:50	353212	G043H7
CCR4	BB700	BD	1:50	566475	1G1
CCR6	BUV737	BD	1:75	612780	11A9
CXCR3	AF647	BioLegend	1:100	353712	G025H7
STEP 3: Stain remaining antibodies at room temperature for 30 minutes in BD Brilliant Stain Buffer Plus.					
Marker	**Fluorophore**	**Supplier**	**Dilution**	**Product number**	**Clone**
CD40L	BV421	BioLegend	1:25	310824	24-31
4-1BB	PE-Cy7	BioLegend	1:25	309818	4B4-1
CD4	BUV496	BD	1:25	612936	SK3
CD14	BV510	BioLegend	1:100	301842	M5E2
CD19	BV510	BioLegend	1:100	302242	HIB19
CD45RA	BV570	BioLegend	1:200	304132	HI100
CD69	BV650	BioLegend	1:50	310934	FN50
CD3	BUV805	BD	1:50	612895	UCHT1
CD8	BUV395	BD	1:250	563795	RPA-T8
STEP 4: Wash and fix cells in 1% paraformaldehyde.					

Table S7. Protocol for surface and intracellular staining for flow cytometry.

STEP 1: Stain for chemokine receptors at 37°C for 10 minutes.					
Marker	**Fluorophore**	**Supplier**	**Dilution**	**Product number**	**Clone**
CCR7	APC-Cy7	BioLegend	1:50	353212	G043H7
CCR4	BB700	BD	1:50	566475	1G1
CCR6	BUV737	BD	1:75	612780	11A9
CXCR3	AF647	BioLegend	1:50	353712	G025H7
STEP 2: Stain surface antibodies and viability at room temperature for 30 minutes in BD Brilliant Stain Buffer Plus.					
Marker	**Fluorophore**	**Supplier**	**Dilution**	**Product number**	**Clone**
PD-1	BV711	BioLegend	1:25	329928	EH12.2H7
CD4	BUV496	BD	1:25	612936	SK3
CD14	BV510	BioLegend	1:100	301842	M5E2
CD19	BV510	BioLegend	1:100	302242	HIB19
CD45RA	BV570	BioLegend	1:200	304132	HI100
CD8	BUV395	BD	1:250	563795	RPA-T8
LIVE/DEAD fixable aqua	For 405 nm excitation	Invitrogen	1:1667	L34957	-
CD38	APC-R700	BD	1:50	564979	HIT2
STEP 3: Fix and permeabilize with FoxP3 Transcription Factor Staining Buffer Set (Invitrogen, #00-5523-00) according to the provided protocol.					
STEP 4: Stain intracellular antibodies at room temperature for 30 minutes in BD Brilliant Stain Buffer Plus and 1X permeabilization buffer.					
Marker	**Fluorophore**	**Supplier**	**Dilution**	**Product number**	**Clone**
CD40L	BV421	BioLegend	1:25	310824	24-31
IL-17A	eFluor660	Invitrogen	1:25	50-7178-42	eBio64CAP17
IL-2	PE-Dazzle594	BioLegend	1:33	500344	MQ1-17H12
4-1BB	PE-Cy7	BioLegend	1:100	309818	4B4-1
TNFa	BV650	BD	1:166	563418	MAb11
CD3	BUV805	BD	1:250	612895	UCHT1
CD69	BUV563	BD	1:200	748764	FN50
IFN-γ	PE	BioLegend	1:400	506507	B27
Granzyme B	BB790	BD	1:500	624296	GB11
STEP 5: Wash and fix cells in 1% paraformaldehyde.					

Table S8. Protocol for tetramer, surface and intracellular staining for flow cytometry.

STEP 1: Incubate with Dasatinib at room temperature for 10 minutes.					
Reagent	**Fluorophore**	**Supplier**	**Final conc.**	**Product number**	**Clone**
Dasatinib	-	Stemcell	50µM	73082	-
STEP 2: Incubate with one relevant PE tetramer/tetramer pool at room temperature for 20 minutes. Each tetramer should be equivalent to 0.2µl of pMHC (0.5ug/ml).					
Reagent				**Fluorophore**	
Tetramer pool consisting of: SARS-CoV-2 nucleocapsid A*0201 LLLDRLNQL SARS-CoV-2 ORF3a A*0201 ALSKGVHFV SARS-CoV-2 ORF3 A*0201 LLYDANYFL				PE	
SARS-CoV-2 nucleocapsid B*0702 SPRWYFYYL				PE	
CMV B*0702 TPRVTGGGAM				PE	
CMV A*0201 NLVPMVATV				PE	
STEP 3: Incubate with one relevant BV421 tetramer at room temperature for 20 minutes.					
Reagent				**Fluorophore**	
SARS-CoV-2 spike A*0201 YLQPRTFLL				BV421	
SARS-CoV-2 spike A*2402 QYIKWPWYI				BV421	
SARS-CoV-2 spike B*0702 SPRRARSVA				BV421	
CMV A*0201 NLVPMVATV				BV421	
STEP 4: Wash cells. Stain for viability at room temperature for 10 minutes.					
Marker	**Fluorophore**	**Supplier**	**Dilution**	**Product number**	**Clone**
LIVE/DEAD fixable aqua	For 405 nm excitation	Invitrogen	1X in PBS	L34957	-
STEP 5: Stain for chemokine receptors at 37°C for 10 minutes.					
Marker	**Fluorophore**	**Supplier**	**Dilution**	**Product number**	**Clone**
CCR7	APC-Cy7	BioLegend	1:50	353212	G043H7
CXCR3	PE-Cy5	PE-Cy5	1:200	353756	G025H7
CX3CR1	BUV615	BUV661	1:100	750690	2A9-1
STEP 6: Stain surface antibodies at room temperature for 30 minutes in BD Brilliant Stain Buffer Plus.					
Marker	**Fluorophore**	**Supplier**	**Dilution**	**Product number**	**Clone**
CD8	BUV396	BioLegend	1:200	563795	RPA-T8
CD38	BUV496	BD	1:200	612946	HIT2
LAG3	BUV661	BD	1:200	624285	T47-530
PD-1	BUV737	BD	1:50	612791	EH12.1
CD3	BUV805	BD	1:50	612895	UCHT1
CD14	BV510	BioLegend	1:100	301842	M5E2
CD19	BV510	BioLegend	1:100	302242	HIB19
CD45RA	BV570	BioLegend	1:200	304132	HI100
TIM3	BV605	BioLegend	1:100	502936	344823
HLA-DR	BV650	BD	1:100	564231	G46-6
TIGIT	PE-Dazzle594	BioLegend	1:100	372715	A15153G
CD127	BB630	BD	1:100	Custom	HIL-7R-M21
CD27	BV786	BioLegend	1:50	302832	O323
CD4	PE-Cy5.5	Invitrogen	1:400	35-0042-82	RMA-4.5
CD95	BB700	BioLegend	1:50	305634	DX2
CD39	BV711	BioLegend	1:100	328228	A1
STEP 5: Wash and fix cells in 1% paraformaldehyde.					

Table S9. Protocol for surface staining and oligo-conjugated antibody staining for single-cell sorting and sequencing.

STEP 1: Stain for viability at room temperature for 10 minutes.					
Marker	**Fluorophore**	**Supplier**	**Dilution**	**Product number**	**Clone**
LIVE/DEAD fixable aqua	For 405 nm excitation	Invitrogen	1X in PBS	L34957	-
STEP 2: Stain for chemokine receptors at 37°C for 10 minutes.					
Marker	**Conjugate**	**Supplier**	**Dilution**	**Product number**	**Clone**
CCR7	TotalSeq-C0148	BioLegend	1:300	353251	G043H7
CXCR5	TotalSeq-C0144	BioLegend	1:500	356939	J252D4
CXCR3	TotalSeq-C0140	BioLegend	1:500	353747	G025H7
CX3CR1	TotalSeq-C0179	BioLegend	1:500	355705	K0124E1
CCR4	TotalSeq-C0071	BioLegend	1:500	359425	L291H4
CCR5	TotalSeq-C0141	BioLegend	1:500	359137	J418F1
CCR6	TotalSeq-C0143	BioLegend	1:500	353440	G034E3
CXCR6	TotalSeq-C0804	BioLegend	1:500	356023	K041E5
STEP 3: Stain remaining antibodies at room temperature for 30 minutes in BD Brilliant Stain Buffer Plus. Each sample was also stained with a single hashtag antibody.					
Marker	**Fluorophore**	**Supplier**	**Dilution**	**Product number**	**Clone**
CD40L	BV421	BioLegend	1:25	310824	24-31
4-1BB	PE-Cy7	BioLegend	1:25	309818	4B4-1
CD4	FITC	BD	1:25	345768	SK3
CD14	BV510	BioLegend	1:100	301842	M5E2
CD19	BV510	BioLegend	1:100	302242	HIB19
CD69	BV650	BioLegend	1:50	310934	FN50
CD8	BV711	BioLegend	1:50	301044	RPA-T8
Marker	**Conjugate**	**Supplier**	**Dilution**	**Product number**	**Clone**
CD4	TotalSeq-C0072	BioLegend	1:1250	300567	RPA-T4
CD8	TotalSeq-C0046	BioLegend	1:10000	344753	SK1
CD45RA	TotalSeq-C0063	BioLegend	1:4000	304163	HI100
CD127	TotalSeq-C0390	BioLegend	1:333	351356	A019D5
CD27	TotalSeq-C0154	BioLegend	1:500	302853	O323
PD-1	TotalSeq-C0088	BioLegend	1:500	329963	EH12.2H7
ICOS	TotalSeq-C0171	BioLegend	1:500	313553	C398.4A
HLA-DR	TotalSeq-C0159	BioLegend	1:500	307663	L243
CD122	TotalSeq-C0246	BioLegend	1:500	339021	TU27
CD28	TotalSeq-C0386	BioLegend	1:500	302963	CD28.2
CD95	TotalSeq-C0156	BioLegend	1:500	305651	DX2
CD38	TotalSeq-C0389	BioLegend	1:500	303543	HIT2
CD71	TotalSeq-C0394	BioLegend	1:500	334125	CY1G4
Hashtag	**Conjugate**	**Supplier**	**Dilution**	**Product number**	**Clone**
Hashtag 1	TotalSeq-C0251	BioLegend	1:100	394661	LNH-94; 2M2
Hashtag 2	TotalSeq-C0252	BioLegend	1:100	394663	LNH-94; 2M2
Hashtag 3	TotalSeq-C0253	BioLegend	1:100	394665	LNH-94; 2M2
Hashtag 4	TotalSeq-C0254	BioLegend	1:100	394667	LNH-94; 2M2